RA TEN
ICN PITEŞTI
INSTITUTUL DE CERCETĂRI NUCLEARE

Materials for Gen IV Reactors

Vasile RADU
RATEN Institute for Nuclear Research, Pitesti

Table of Content

I. Material Requirements and Candidate materials for Heavy Liquid Metal Cooled Fast Reactors

Materials requirements for the innovative reactor systems (1)

The main requirements for the materials to be used in these reactor systems are the following:

- The in-core materials need to exhibit dimensional stability under irradiation, whether under stress (irradiation creep or relaxation) or without stress (swelling, growth).
- The mechanical properties of all structural materials (tensile strength, ductility, creep resistance, fracture toughness, resilience) have to remain acceptable after ageing.
- The materials have to retain their properties in corrosive environments (reactor coolant or process fluid).

Other criteria for the materials are their costs to fabricate and to assemble, their composition should be optimized in order for instance to present low-activation (or rapid deactivation) features which facilitate maintenance and disposal.

These requirements have to be met under normal operating conditions, as well as in incidental and accidental conditions.

Materials requirements for the innovative reactor systems (2)

- These demands are similar in their nature to those required for the current operating commercial reactors, but are actually much more demanding, due to the specifications of the innovative systems.
- It can be noted that, when the operating temperature of commercial light water reactors does not exceed 625 K, the levels of temperature required here are much higher as illustrated which represents a major challenge.

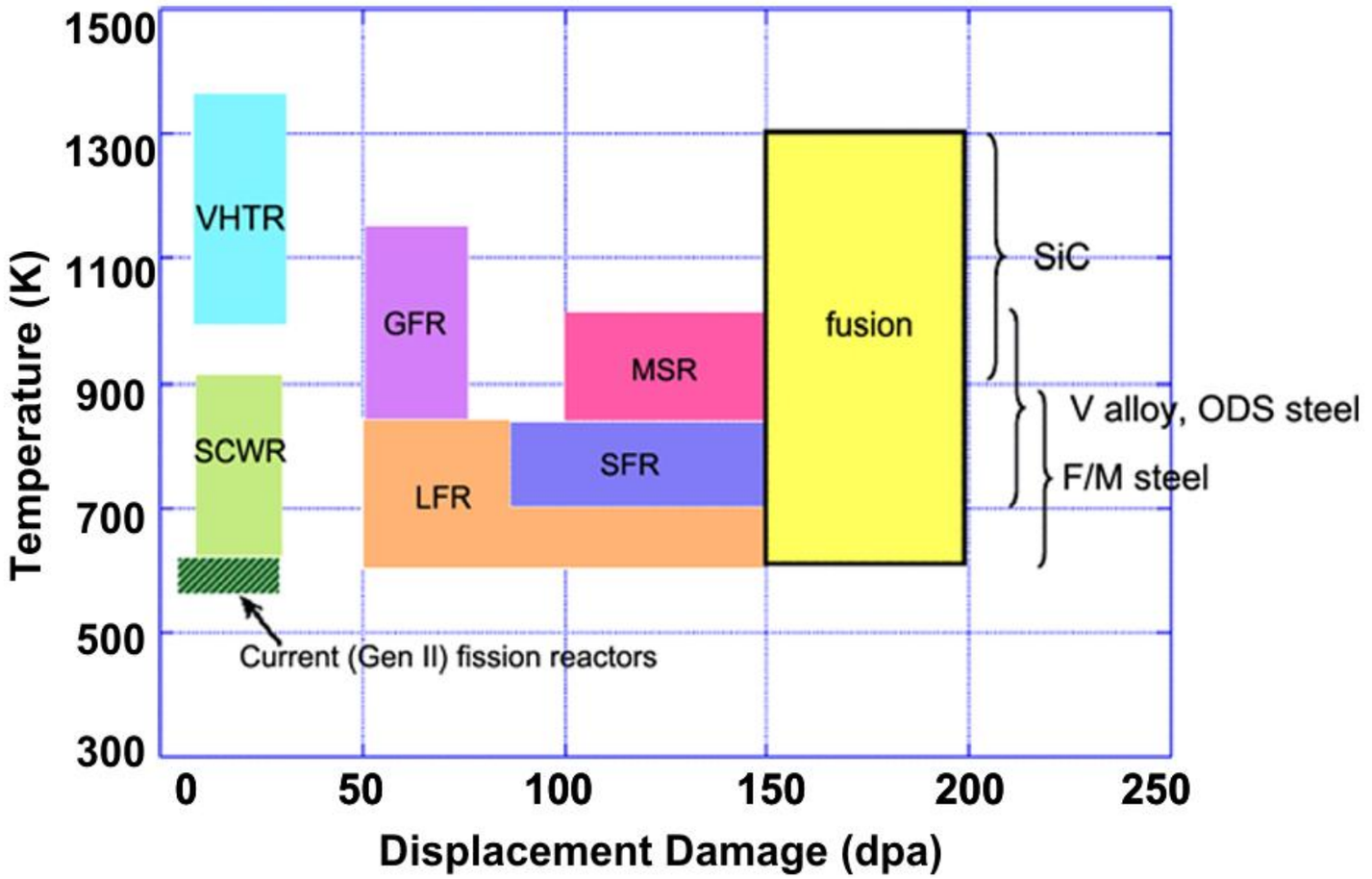

Operating temperature as a function of displacement dose for different reactor systems

Materials requirements for the innovative reactor systems (3)

- Another tough challenge is the high irradiation doses sustained by the in-core materials. Also, it can be difficult to find materials compatible with some of the coolant or process fluids considered.
- The combination of high temperature, high neutron dose and environment could prove to be a major obstacle for the viability of some of the systems.
- Finally, the toughest demand is the lifetime expectancy, which is 60 years, where the maximum design life of reactor materials is more in the range of 30 years

	SFR	GFR	LFR
Coolant	Liquid Na	He	Lead alloys
P (MPa)	0.1	7	0.1
T (K)	625–825	755–1125	825–1075
Core structures	Wrapper F/M steels	Fuel & core structures	Target, Window Cladding
	Cladding Adv Aust & F/M steels		
	F/M ODS	SiC_f/SiC composite	F/M steels ODS
T (K)	665–975	875–1475	625–755
Displacement dose (dpa)	Cladding 200	60 = 90	Cladding ~00 dpa, ADS/ target ~100 dpa
Other components		IHX or turbine Ni alloys	

Summary of materials considered for the different systems

Candidate materials for innovative reactor systems (1)

Ferritic/martensitic steels

- Ferritic/martensitic steels (9–12% Cr) are promising candidate materials for sodium or lead cooled reactors with a high temperature (<875 K) and compact primary system, as well as for the pressure vessel of high temperature gas-cooled reactors.
- There is a strong push to reach high burn ups to optimize the use of resources and to minimize the waste, and the swelling of alloys currently used for fuel cladding in fast neutron reactors limits the burn up, because of geometrical constraints and also the loss of mechanical strength.
- This limitation could be overcome with improved materials such as ferritic/martensitic steels which exhibit a much lower swelling as shown in Fig. which shows that the maximum hoop deformation of austenitic steels increases rapidly after an “incubation” period when that of F/M steels remains low even at displacement doses above 150 displacements per atom (dpa).

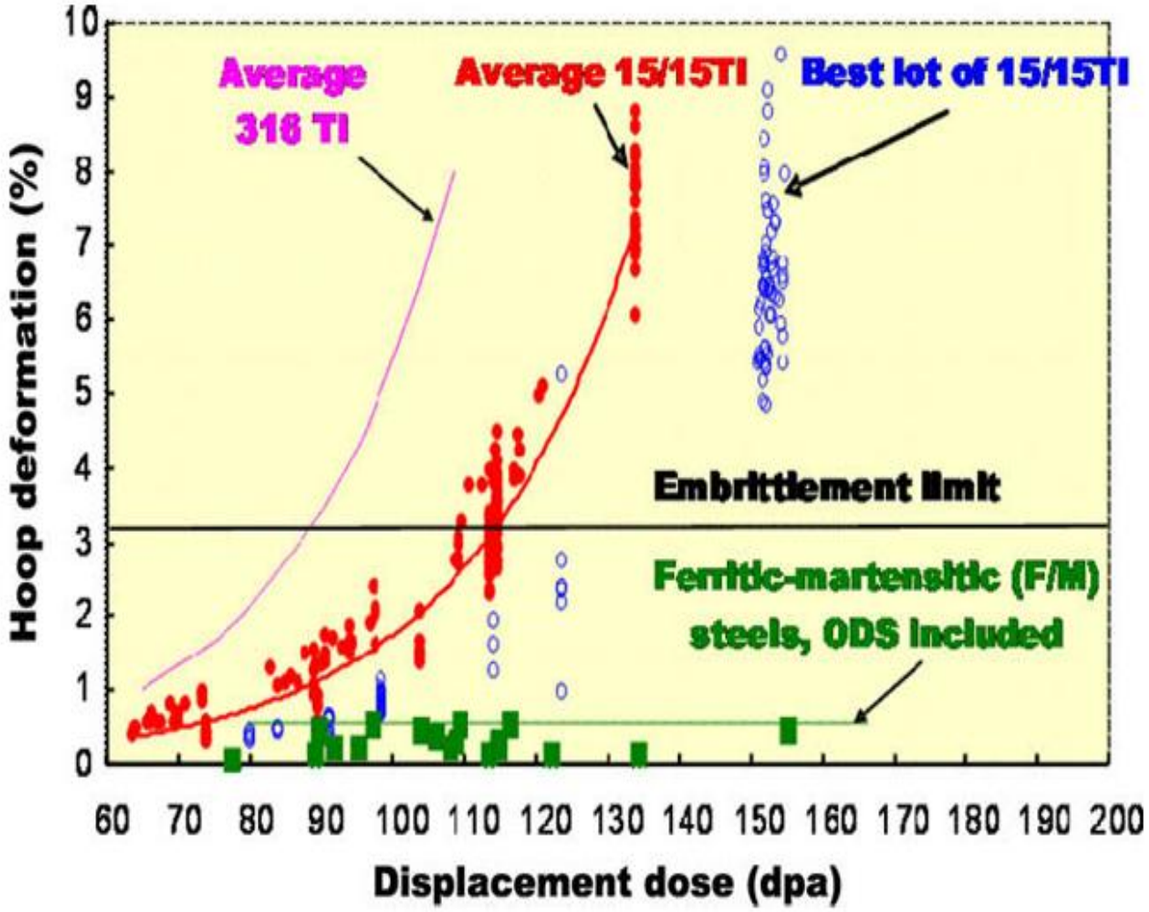

Maximum hoop deformation of different grades of austenitic Phénix claddings and ferrito-martensitic materials versus dose at temperatures between 675K and 825K

Candidate materials for innovative reactor systems (2)

Ferritic/martensitic steels

- Austenitic steels like AISI 316L that are used in water cooled reactors are not only susceptible to irradiation induced swelling and creep, but also show limited corrosion resistance in Pb-alloys at high temperature. Ferritic–martensitic steels have better corrosion behaviour in liquid Pb-alloys than austenitic steels. They also present a better behaviour under irradiation and thus appear to be candidate materials for fuel cladding and structures in high flux zones.

- The 9%Cr martensitic steels with their Low Activation (LA) variants for fusion are foreseen for operating temperatures up to 825 K. A large set of data issued from the various Fast Neutron Reactors programmes exist for the classical 9–12% Cr martensitic steels for doses 100dpa in the range 675–825K.

- The resistance to swelling is excellent due to the bcc crystalline structure and the high density of sinks of the martensitic microstructure. The hardening and embrittlement are negligible when irradiation occurs in the range 675–825 K.

- Finally, these alloys exhibit better mechanical properties, lower thermal dilation and are cheaper than alloys used previously in the intermediary circuit of sodium cooled fast reactors, which would help design a much more compact circuit and make the system more competitive economically.

Candidate materials for innovative reactor systems (3)

Oxide dispersion strengthened steels

- Oxide dispersion strengthened ferritic/martensitic steels are considered for cladding materials for high burn-up fast neutron reactor fuels.
- Figure shows the benefits of a ferritic/martensitic matrix with respect to swelling problems. The nanosized dispersoids of yttrium oxide give these alloys a good creep resistance at high temperatures.
- The ODS grades currently developed in the frame of the SFR or fusion contain 9–12% Cr.
- However, these alloys could show some limitations in terms of internal corrosion (oxide clad reaction) and temperature (phase transition around 1075 K).
- Therefore, ferritic steels with 14% Cr and more could be used up to 1175 K. Although irradiation data are scarce, the bcc crystalline structure should present an excellent resistance to swelling.

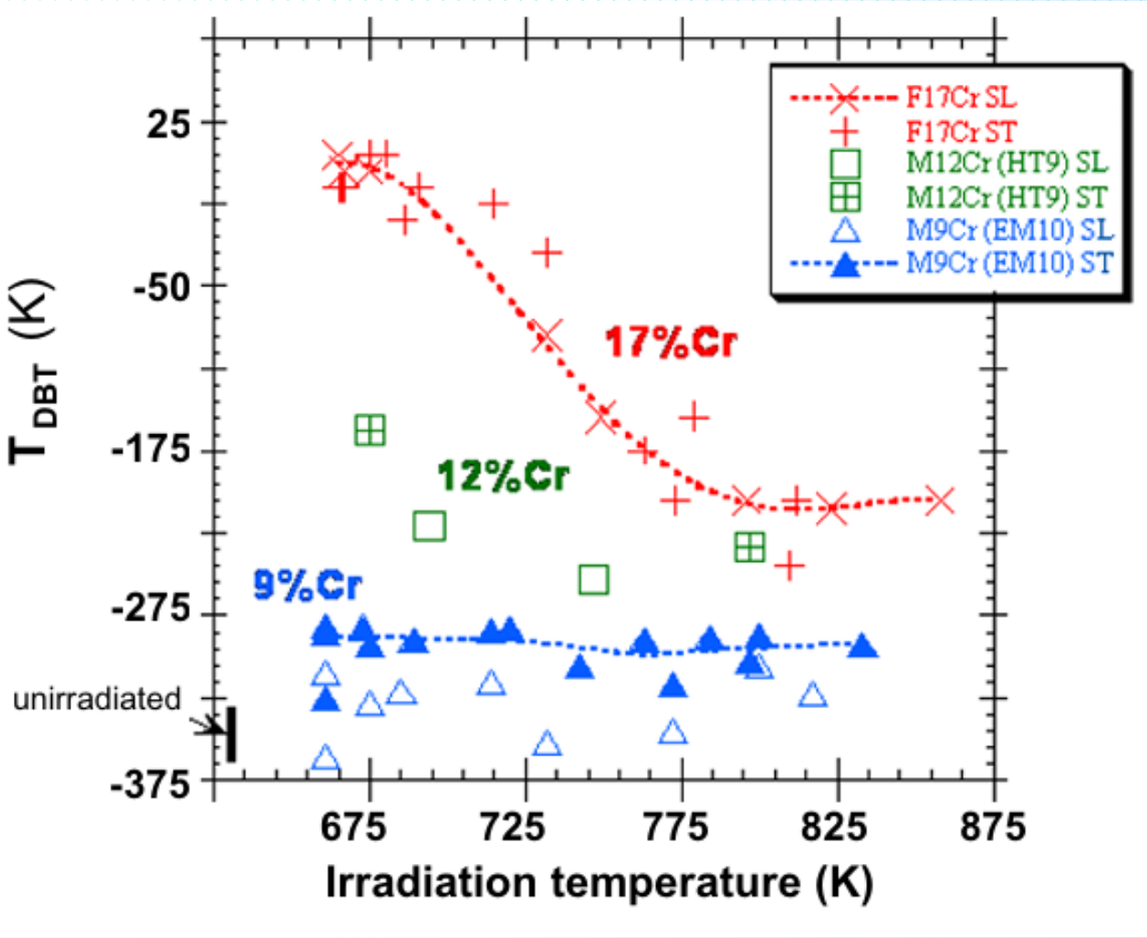

Ductile to brittle transition temperature (TDBT) for F/M steels with different Cr contents as a function of irradiation temperature

Candidate materials for innovative reactor systems (4)

Ceramic materials

- Ceramic materials are needed for very high temperature components (>1275 K) such as heat exchangers and thermal insulations in the primary system, as well as core components such as control rod sheath (V/HTR and GFR) and fuel constituents (GFR as shown in Figure).
- The main goals of the studies on non metallic materials such as graphite or ceramic matrix composites (C/C, C/SiC, SiC/SiC) are to select and characterize various core materials for structural applications (reflectors, fuel structures, control rod cladding, core's support plates) at high temperatures (T =1375K up to 1875K in accidental conditions) under irradiation and impure helium environment.

SiC/SiC fuel pin or fuel plate for GFR

II. RATEN ICN research activities concerning on the Liquid metal embrittlement (LME)

II.1 Overview oh the Liquid Metal Embrittlement phenomenon (LME) (1)

- In the research area for the Generation IV nuclear reactors, a vital task is to manage the structural integrity of the nuclear components under representative environment conditions.
- The damaging factors as irradiation, high temperature and corrosion, constitutes a priority even from the design stage. In the literature the degradation mechanisms of the mechanical properties by liquid metals were mainly classified as LME, liquid metal-assisted damage (LMAD) and environmentally assisted cracking (EAC). Common features of those degradation mechanisms involve a physico-chemical and mechanical process connected with the wetting phenomenon.
- It seems that no single mechanism appears to control LME. Also, a good sort of conflicting results possibly originates from the characteristics of the testing procedure.
- Moreover, a major gap exists between the atomistic simulations at the nanometer level and experimental results at the macroscopic level.

II.1 Overview oh the Liquid Metal Embrittlement phenomenon (LME) (2)

- The subsequent definition for the liquid metal embrittlement is accepted: ***LME is the loss of tensile ductility of stressed normally ductile metals or metallic alloys in contact with a liquid metal that may lead to brittle fracture.***

- LME is taken into account as a specific sort of a case of brittle fracture, inter-granular or trans-granular, by cleavage and it is among little or no penetration of the embrittling atomic species into the solid metal.

- LME behaviour is strongly influenced by the variables affecting material (e.g., solid metal microstructure and chemistry), stress state (e.g., notched vs. smooth bars) and environment (including the numerous factors that affect wetting), which underlines the importance of test conditions on the LME phenomenon.

- The need for LME modelling of stainless-steel systems is emphasised in the scientific dedicated literature. In the meantime, the lack of models, in this case, is owing to the complexity of modelling a multi-component engineering alloy (in opposition to a pure material).

- Taking under consideration the resistance of stainless steels to LME, modelling can be instructive to the overall understanding of LME resistance, but also to use it in the practical applications associated with assessing the structural integrity for the systems in Generation IV reactors.

II.1 Overview oh the Liquid Metal Embrittlement phenomenon (LME) (3)

- Thus, the purpose of the works performed at ICN is to highlight the changes in the thermomechanical behaviour induced by the contact between the 316L austenitic steel with liquid lead, as well as its modelling through the equation of the Ramberg-Osgood-type mechanical stress-strain curve.

- It should be noted that there are still no systematic studies in the specialized literature carried out for the evaluation of the thermomechanical behaviour of 316L steel under tensile mechanical stress in the liquid lead environment, in the range of temperatures 350C – 400C.

Model	The main features	Model support	Limitations	Constitutive equation $\sigma \sim \varepsilon$
Reduction in Surface Energy	Thermodynamic approach, the defect is usually intergranular	Experimental support, consider the effects of experimental observations	Does not take into account the mechanisms of atomic degradation	No
Adsorption Induced Reduction in Cohesion	Adsorption of liquid metal reduces the strength of cohesion on the atomic planes	Qualitatively consider the effects of many experimental observations Fractographic support	No more experimental observations can be explained	No
Enhanced Dislocation Emission	Defect occurs by localized micro- ductile coalescence	Experimental support, strong fractographic support	No math analysis, based on complicated fractographic analyzes	No
Enhanced Work Hardening	Adsorption of liquid metal atoms facilitates dislocation motion	Experimental support for discontinuous crack growth	No math analysis, Lack of experimental support for improved hardening	No
Localized plasticity that favors LME	Liquid metal diffuses along the grain boundary before the crack tip	Correctly predicts that LME rupture is accompanied by extensive plasticity	Lack of experimental support	No
Dissolution-Condensation	Crack growth by the stress-assisted dissolution of solid metal into liquid metal at the tip of the crack	Limited experimental support	Predicts the wrong dependence of LME on the composition of liquid metals	No
Grain Boundary Penetration	Promoted stress diffusion of the liquid metal along the grain boundaries before the crack tip	Can qualitatively consider the effects of many experimental observations,	No math analysis, lack of experimental support	No
Present study	**Adsorption of liquid metal reduces the strength of cohesion in front of microcracks**	**Experimental support, strong fractographic support**	**Does not take into account the oxygen effect in the liquid lead on LME**	**Yes Ramberg-Osgood**

II.2 Slow strain rate testing of 316l stainless steel in the air and in the liquid lead environment (1)

- The experimental tests on the 316L stainless steel specimens, used in Generation IV reactors were performed in both the liquid lead and the air environment to highlight better the material behaviour under the liquid metal embrittlement.
- In this regard, it was preferred the Slow Strain Rate Test (SSRT). According to ASTM - G129-00 the SSRT is used for the relatively screening or comparative evaluation of environmental variables, that can affect the resistance of a material to environmentally assisted cracking. (EAC). The slow constant extension rate produces a gage section strain rate, which is usually in the range from 10^(−4) to 10^(−7) s-1 .
- The SSRT is a comparative evaluation and therefore it was conducted in two environments: (1) one in which the material under evaluation is not susceptible to EAC (air), and (2) the other in which the resistance to EAC of the material is being determined (liquid lead).

II.2 Slow strain rate testing of 316l stainless steel in the air and in the liquid lead environment (2)

- An important facility has been designed and built up for the Instron Testing Facility (Fig. (a)) for the liquid lead experiments.
- The Walter+Bai Machine (Fig. (b)) allows the tensile tests in the air.
- Also, one may see the typical specimen aspect before and after testing in the liquid lead in Fig. (c), respectively Fig. (d).

(a)

(b)

(c)

(d)

Figure a) Instron Testing Facility for SSRT in the liquid lead; b) Walter+Bai Machine in the air; c) 316L specimen before testing; d) 316L specimen after testing

II.2 Slow strain rate testing of 316l stainless steel in the air and in the liquid lead environment (3)

- The tensile tests in air and liquid lead were carried out at deformation rates of the sample in the range 10^(-3) s-1 ~ 10^(-5) s-1, following ASTM G129 and ASTM E8, in a temperature range of 350°C - 400°C.
- The diagrams obtained during the "Slow Strain Rate Testing" (SSRT) tests were converted into real mechanical stress-strain curves.
- Figure shows a set of curves σ=f(ε), which were represented up to the necking points of interest, points where the tangents to these curves take zero value.

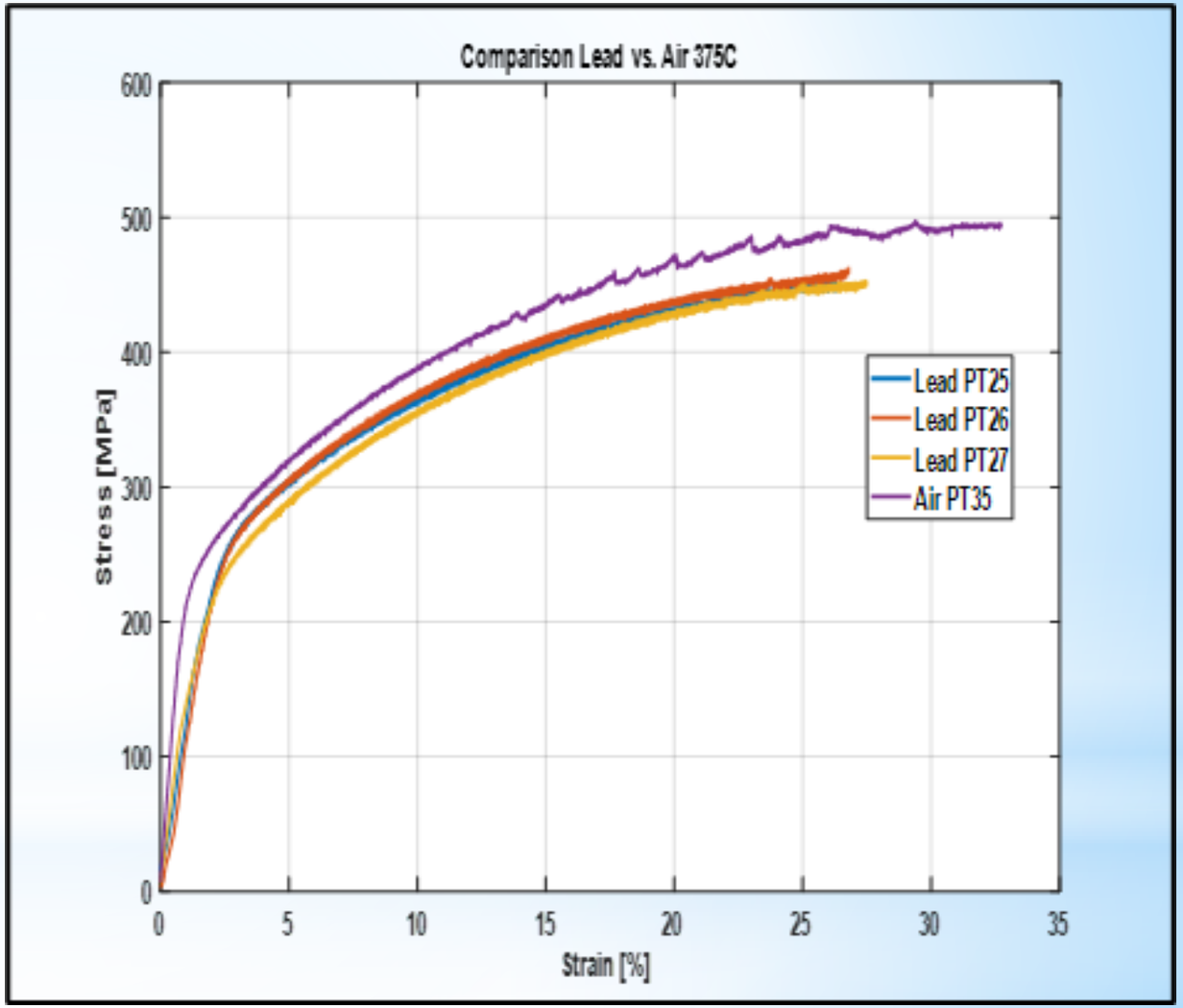

II.2 Slow strain rate testing of 316l stainless steel in the air and in the liquid lead environment (4)

SEM

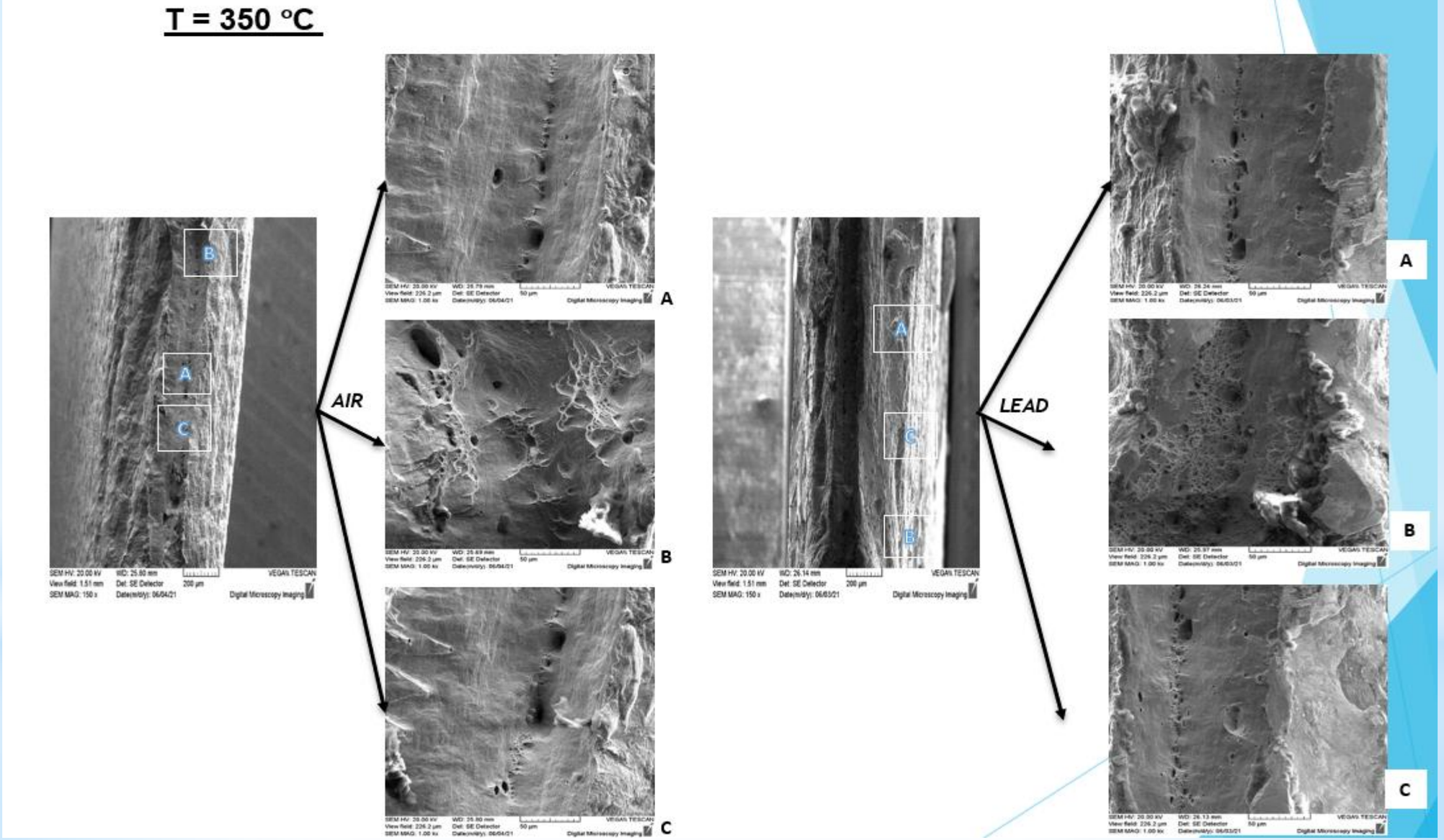

II.2 Slow strain rate testing of 316l stainless steel in the air and in the liquid lead environment (5)

SEM

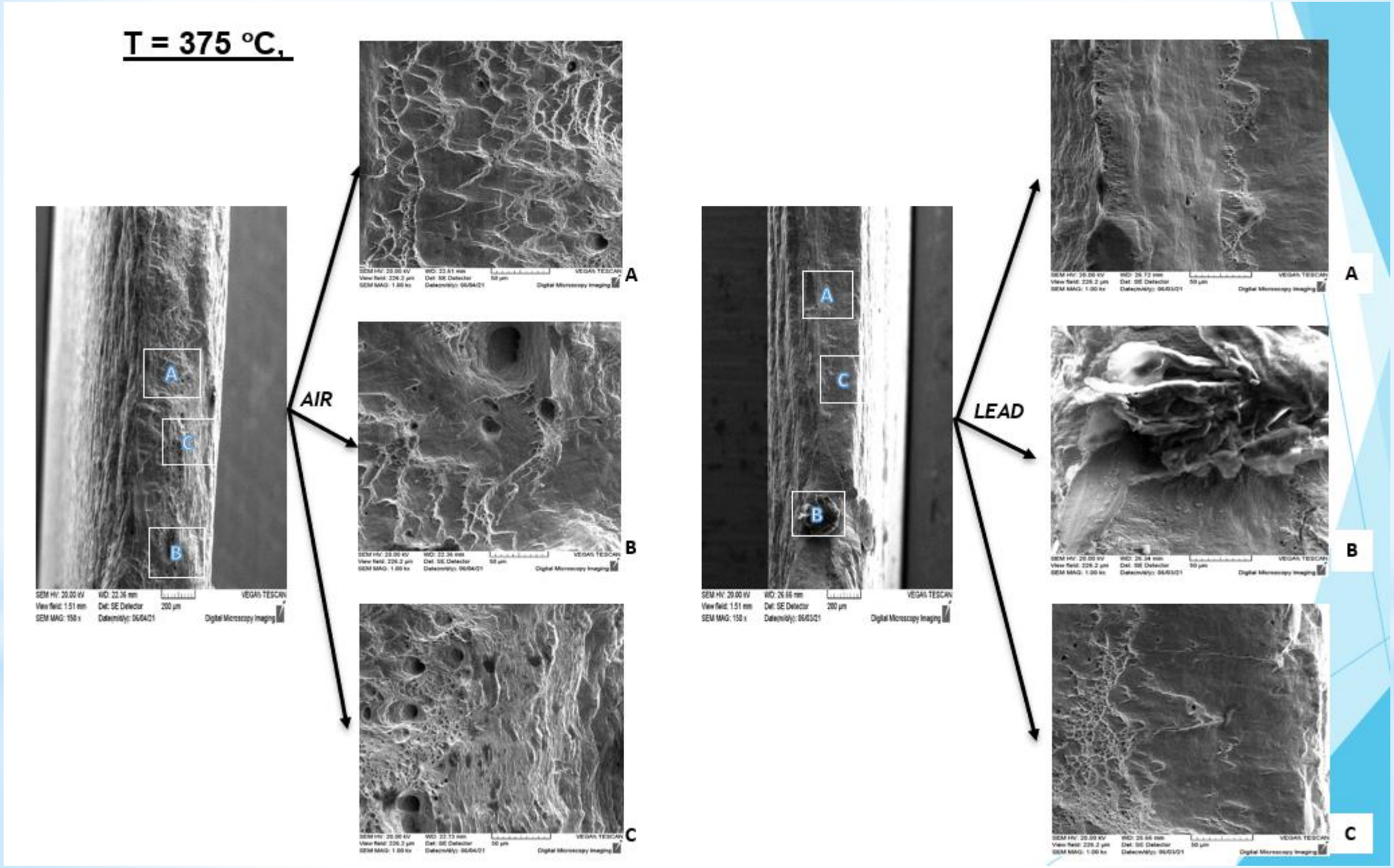

II.2 Slow strain rate testing of 316l stainless steel in the air and in the liquid lead environment (6)

SEM

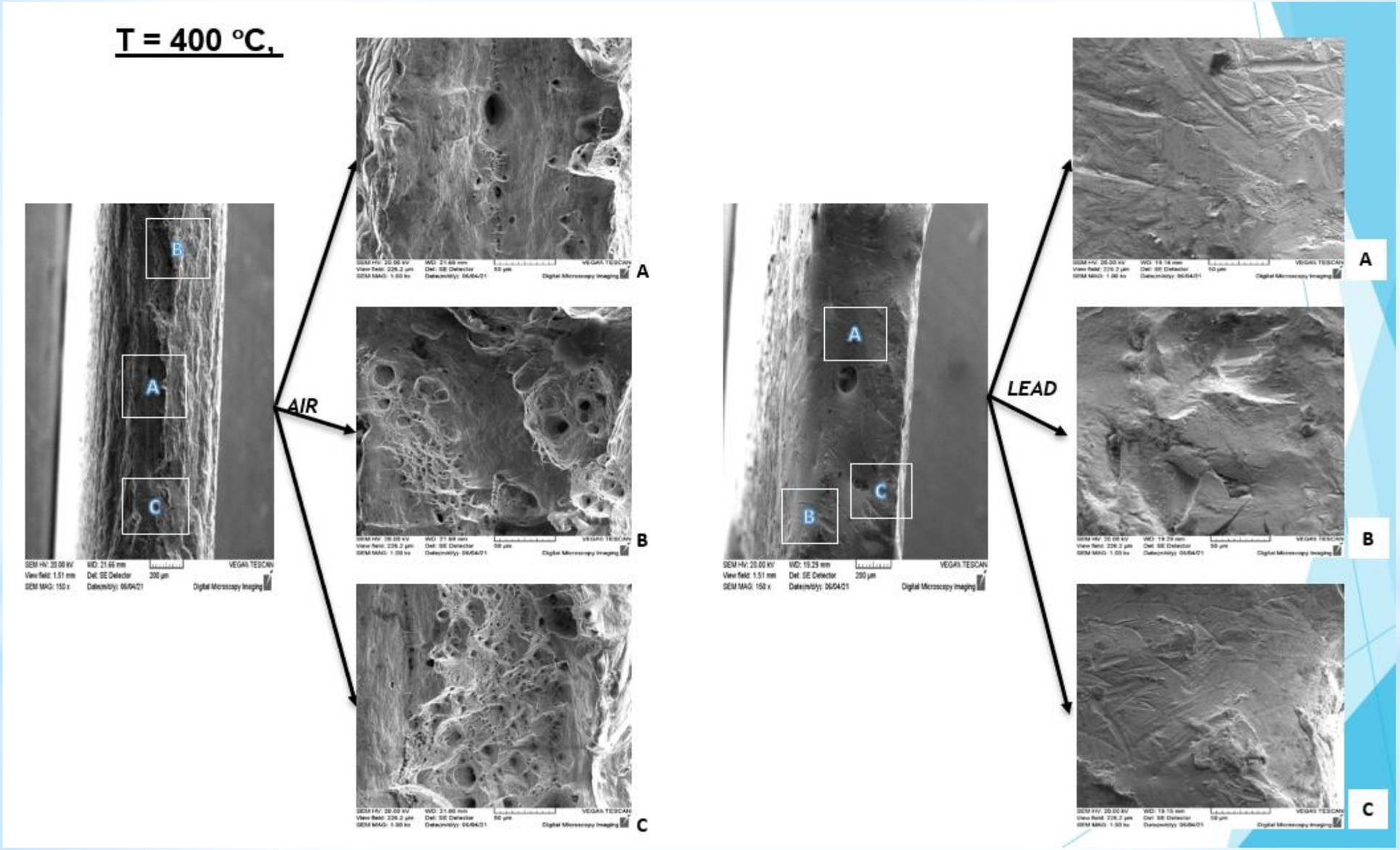

II.2 Slow strain rate testing of 316l stainless steel in the air and in the liquid lead environment (7)

- The experimental tensile mechanical tension-deformation curves will be processed according to the Ramberg - Osgood model.
- From practical considerations, related to the use of the constitutive equation in the analysis with the finite element method, the equation of the stress-strain curve in the Ramberg – Osgood format has the form:

$$\frac{\varepsilon}{\varepsilon_0} = \frac{\sigma}{\sigma_0} + \alpha \cdot \left(\frac{\sigma}{\sigma_0}\right)^m$$

- It is characterized by parameters α , respectively m=1/n, which is the inverse of the hardening exponent.
- Using a specific methodology described in some own papers, from the curves σ=f(ε) the following quantities were extracted: the coefficient α of the Ramberg-Osgood relation, the parameter m, which is the inverse of the hardening exponent, n.
- At the same time, the database also contains the yield stress values, σ0.2 , respectively of the maximum stress corresponding to the localized deformation, σu , which were determined for all tested specimens.

II.2 Slow strain rate testing of 316l stainless steel in the air and in the liquid lead environment (8)

- The values obtained for the coefficient α of the Ramberg-Osgood relationship following tests performed **in the air** on 316L stainless steel samples, as well as the parameter m, which is the inverse of the hardening exponent, n; depending on the strain rate in the temperature range 350°C - 400°C in air.
- For the coefficient α of the Ramberg - Osgood equation, for the entire temperature range (350°C – 400°C), the value of the parameter α increases slightly with the increase of the strain rate; with the increase in temperature, regardless of the strain rate, the value of the parameter decreases.
- For the parameter m of the Ramberg – Osgood equation, for the entire temperature range (350°C – 400°C), the value of the parameter m increases slightly with the increase of the strain rate; with increasing temperature, regardless of the deformation rate, the value of the parameter increases.

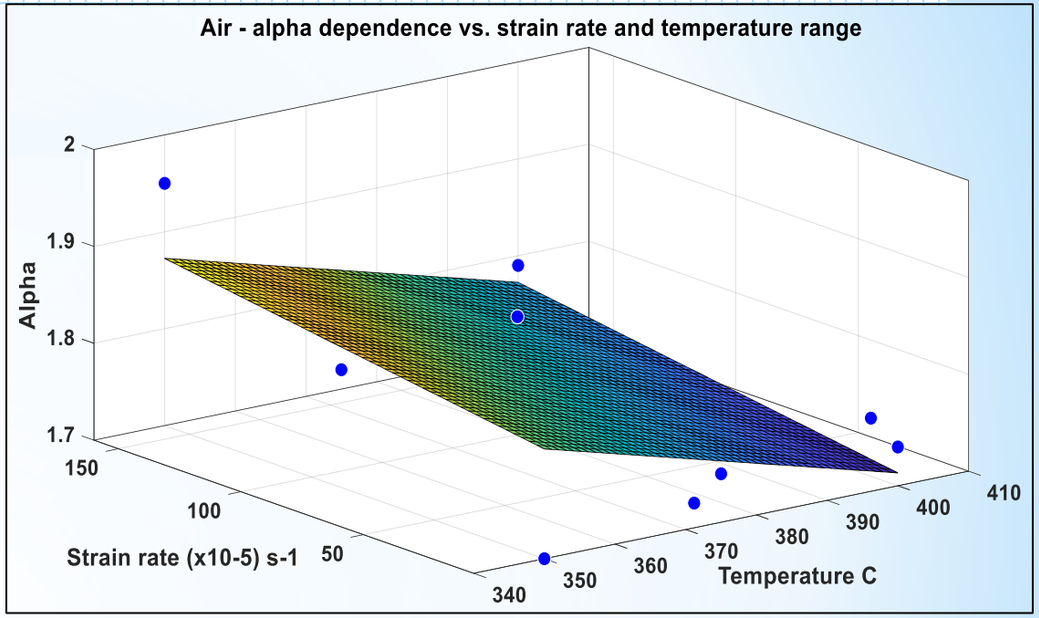

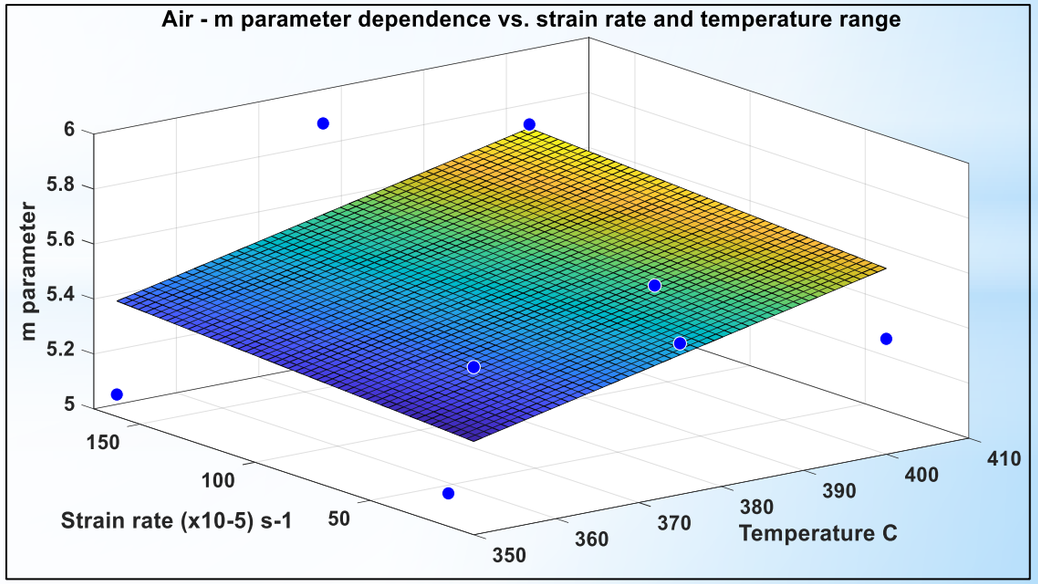

II.2 Slow strain rate testing of 316l stainless steel in the air and in the liquid lead environment (9)

- The values obtained from the tests performed **in the liquid lead** environment on 316L stainless steel samples for the coefficient α of the Ramberg-Osgood relationship, and the parameter m, which is the inverse of the hardening exponent, n.
- For the parameter α of the Ramberg-Osgood equation, in the tests performed in liquid lead, for the entire temperature range (350°C - 400°C), the value of the parameter α remains almost constant at each value of the strain rate; The same can be said for the dependence of the strain rate at a given temperature value.
- For the parameter m of the Ramberg - Osgood equation, in the tests performed in the liquid lead for the entire temperature range (350°C – 400°C), the value of the parameter m decreases significantly with the increase of the deformation speed; With increasing temperature, the value of the parameter m remains almost constant for a given value of the strain rate.

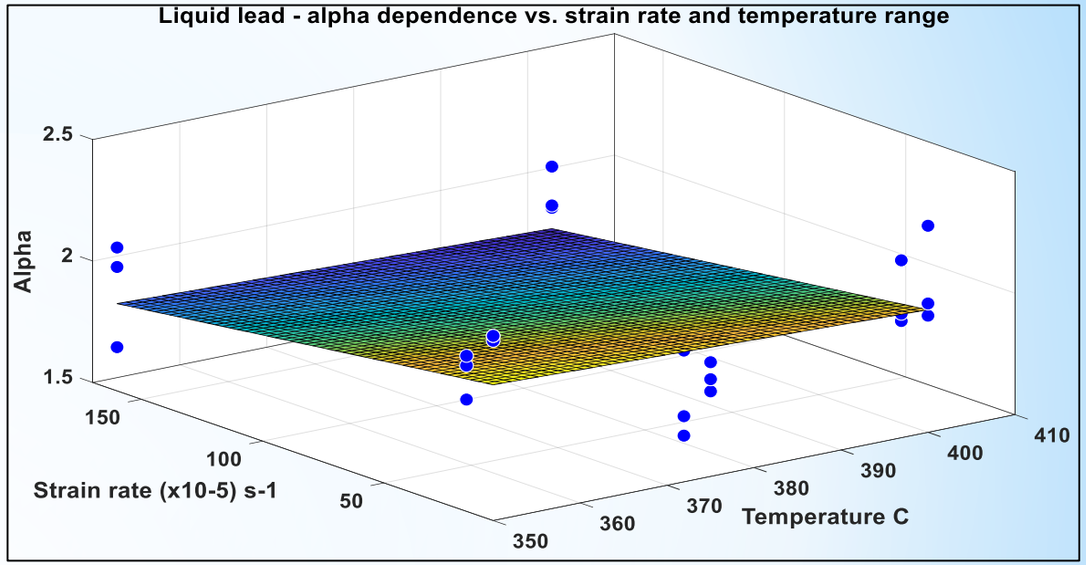

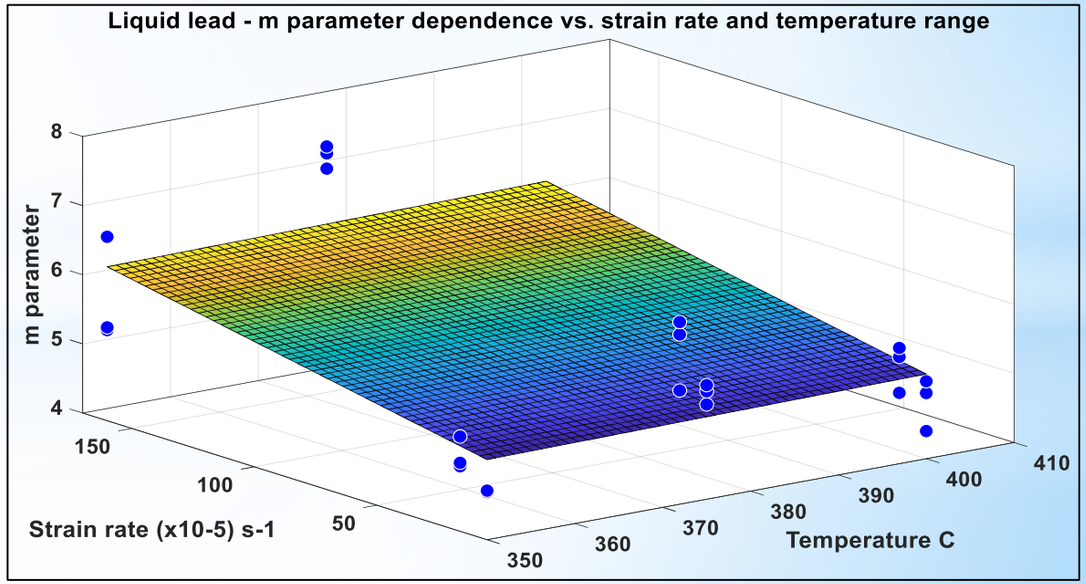

II.2 Slow strain rate testing of 316l stainless steel in the air and in the liquid lead environment (10)

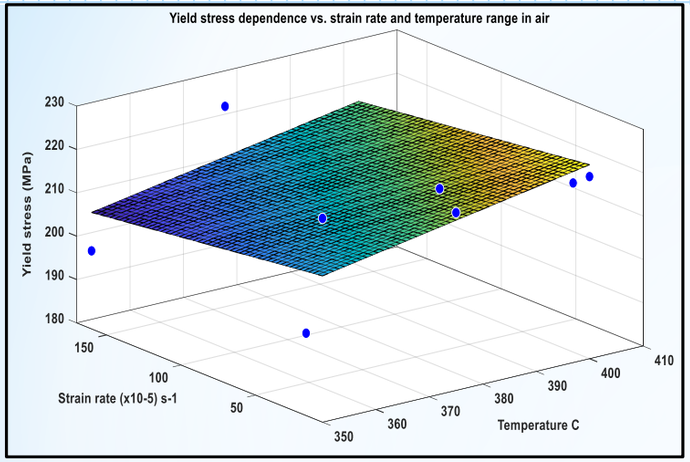

(a)

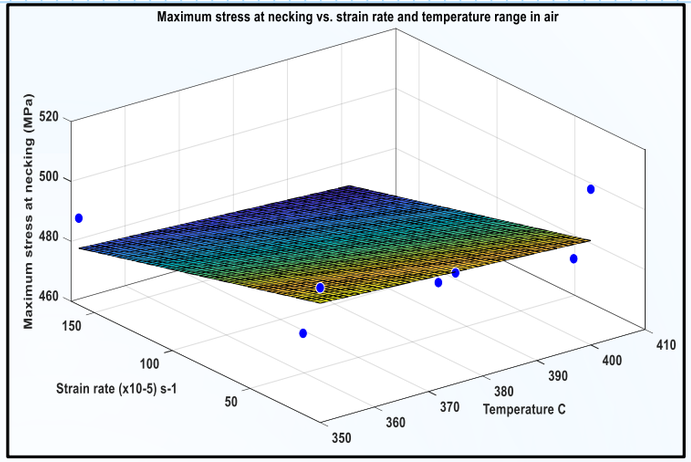

(b)

Yield stress (a) and maximum stress corresponding to localized deformation (b), for 316L steel depending on the strain rate in the temperature range 350°C - 400°C in air.

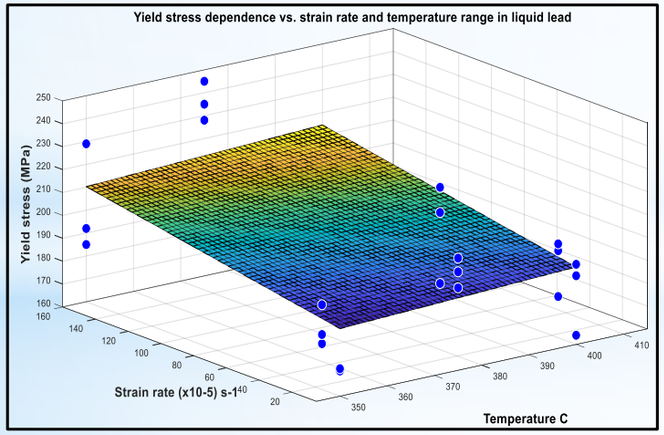

(a)

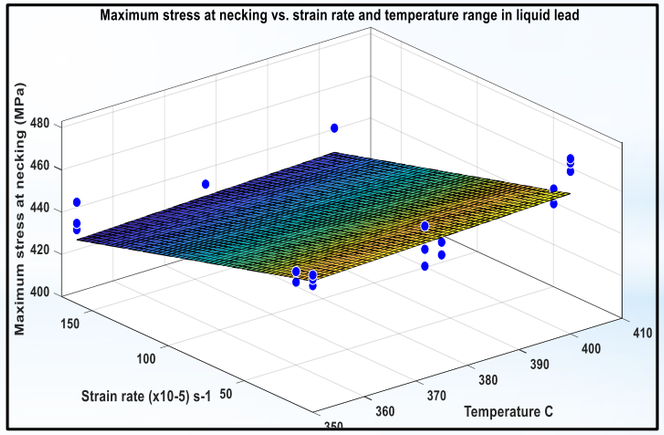

(b)

Yield stress (a) and maximum stress corresponding to localized deformation (b), for 316L steel depending on the strain rate in the temperature range 350°C - 400°C in the liquid lead.

II.3 Multilayer feedforward neural network used to model the parameters for ramberg-osgood stress-strain curve equation (1)

- In function approximation, the Multilayer Feedforward Neural Network (MFNN) is probably the most popular network architecture used in nonlinear neural modelling today.
- In this type of network, each unit takes a weighted sum of the input data and passes this activation level through a transfer function.
- Input data is processed through a one-way network, "forward", passing through successive layers. Figure shows a simplified flaw chart used for a two-layer tansig/purelin MFNN network.

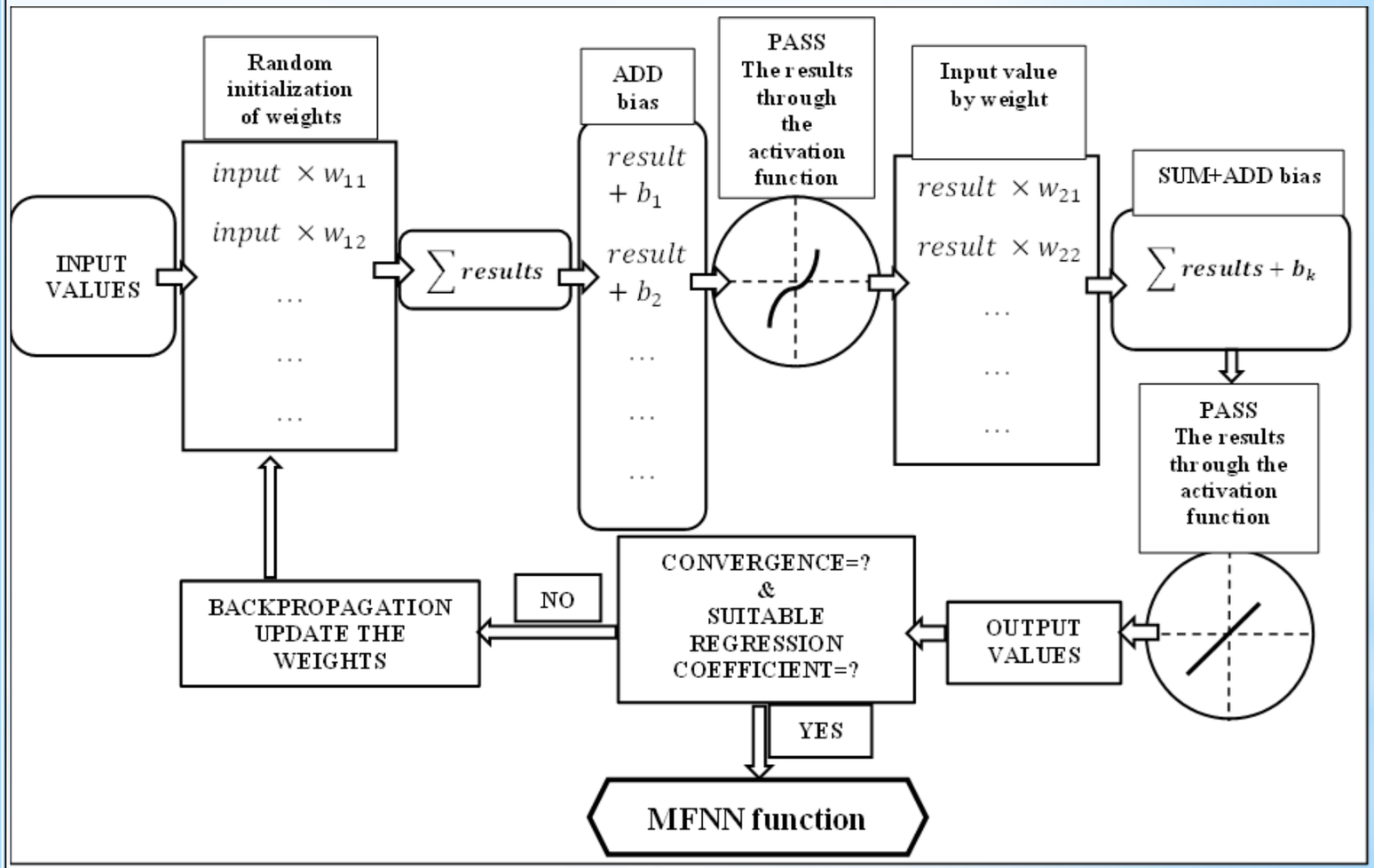

II.3 Multilayer feedforward neural network used to model the parameters for ramberg-osgood stress-strain curve equation (2)

$$\alpha_{air}(T,\dot{\varepsilon},\sigma_{0.2},\sigma_u) = \\ = \frac{0.1535199832}{\exp(0.0157169072\cdot\sigma_{0.2} - 0.06676656384\cdot\sigma_u - 0.07362022963\cdot T - 0.1083065326\cdot\dot{\varepsilon} + 75.29003156) + 1.0} \\ - \frac{0.2365077134}{\exp(0.04264235719\cdot\sigma_u - 0.4544772243\cdot\sigma_{0.2} - 0.00392211372\cdot T - 0.008434048107\cdot\dot{\varepsilon} + 79.34997665) + 1.0} \\ + \frac{0.6325132439}{\exp(50.14925053 - 0.07986180668\cdot\sigma_u - 0.234652205\cdot T - 0.05375160671\cdot\dot{\varepsilon} - 0.03426597872\cdot\sigma_{0.2}) + 1.0} \\ - \frac{2.076965747}{\exp(0.5050429755\cdot\sigma_{0.2} + 0.2481844408\cdot\sigma_u - 0.3889452763\cdot T + 0.2070418955\cdot\dot{\varepsilon} - 49.10719742) + 1.0} \\ - \frac{2.153155082}{\exp(0.2180445427\cdot\sigma_{0.2} + 0.1479708912\cdot\sigma_u + 0.1207130135\cdot T + 0.07089952978\cdot\dot{\varepsilon} - 123.4715136) + 1.0} \\ + 1.307553795$$

$$\alpha_{lead}(T,\dot{\varepsilon},\sigma_{0.2},\sigma_u) = \\ = \frac{0.01111703549}{\exp(0.1758779686\cdot\sigma_{0.2} - 0.6841160186\cdot\sigma_u + 0.4240382537\cdot T + 0.4211538564\cdot\dot{\varepsilon} + 73.75522087) + 1.0} \\ - \frac{0.4168912674}{\exp(0.4670985643\cdot\sigma_{0.2} - 0.0421241148\cdot\sigma_u + 0.3415910184\cdot T - 0.3131816471\cdot\dot{\varepsilon} + 19.93870722) + 1.0} \\ + \frac{0.9591262485}{\exp(0.04809159409\cdot\sigma_{0.2} + 0.003358524713\cdot\sigma_u - 0.0005350602848\cdot T + 0.0004271396583\cdot\dot{\varepsilon} - 10.41126806) + 1.0} \\ + \frac{0.04771190512}{\exp(1.005654552\cdot\sigma_{0.2} - 0.4563315874\cdot\sigma_u - 0.1039207902\cdot T - 0.0006274577723\cdot\dot{\varepsilon} - 59.20988646) + 1.0} \\ + \frac{1.71252668}{\exp(0.4536180027\cdot\sigma_u - 0.1283652688\cdot\sigma_{0.2} - 0.4198358056\cdot T - 0.01257380184\cdot\dot{\varepsilon} - 56.939743) + 1.0} \\ - 0.195416497$$

$$m_{air}(T,\dot{\varepsilon},\sigma_{0.2},\sigma_u) = \\ = \frac{1.376823648}{\exp(0.1010589155\cdot\sigma_u - 0.00903922038\cdot\sigma_{0.2} - 0.1437156176\cdot T + 0.01072826591\cdot\dot{\varepsilon} - 23.45732203) + 1.0} \\ - \frac{2.290502637}{\exp(0.1350483712\cdot T - 0.03574108429\cdot\sigma_u - 0.1594679465\cdot\sigma_{0.2} - 0.02427346108\cdot\dot{\varepsilon} + 32.53306723) + 1.0} \\ - \frac{3.027996311}{\exp(0.09500214958\cdot T - 0.05144939472\cdot\sigma_u - 0.265195393\cdot\sigma_{0.2} + 0.05112680995\cdot\dot{\varepsilon} + 78.1810692) + 1.0} \\ - \frac{2.71534429}{\exp(0.1816733758\cdot T - 0.1041205667\cdot\sigma_u - 0.09708069808\cdot\sigma_{0.2} - 0.1315849855\cdot\dot{\varepsilon} + 48.45071035) + 1.0} \\ + \frac{2.041644833}{\exp(0.02508797134\cdot\sigma_u - 0.05717042737\cdot\sigma_{0.2} - 0.0004544975416\cdot T - 0.00004444304224\cdot\dot{\varepsilon} + 1.064443306) + 1.0} \\ + 3.508276934$$

$$m_{plumb}(T,\dot{\varepsilon},\sigma_{0.2},\sigma_u) = \\ = \frac{3.643881706}{\exp(0.6385643297\cdot T - 0.2022424958\cdot\sigma_u - 0.6227643831\cdot\sigma_{0.2} - 0.1053848883\cdot\dot{\varepsilon} - 77.21535061) + 1.0} \\ - \frac{9.884337419}{\exp(0.01629318253\cdot\sigma_{0.2} - 0.007234343592\cdot\sigma_u + 0.0007329634094\cdot T + 0.0001456651298\cdot\dot{\varepsilon} - 1.455770771) + 1.0} \\ + \frac{0.08146039906}{\exp(0.4112705698\cdot\sigma_{0.2} - 0.3970669265\cdot\sigma_u - 0.3081988387\cdot T + 0.3491973275\cdot\dot{\varepsilon} + 38.95247934) + 1.0} \\ + \frac{7.106945027}{\exp(0.4026283571\cdot\sigma_{0.2} + 0.4217960215\cdot\sigma_u - 0.8012441872\cdot T + 0.07559427212\cdot\dot{\varepsilon} - 37.3985282) + 1.0} \\ + \frac{1.621509654}{\exp(0.3513192334\cdot\sigma_{0.2} + 0.09960028714\cdot\sigma_u - 0.7307116249\cdot T + 0.2176743567\cdot\dot{\varepsilon} + 69.50970479) + 1.0} \\ + 0.6084863663$$

II.3 Multilayer feedforward neural network used to model the parameters for ramberg-osgood stress-strain curve equation (3)

- Processing of experimental data obtained for 316L steel **in the air environment**. After processing the data through the MFNN network methodology, the functions obtained for the R-O coefficients are $\alpha_{air}\ (T, \dot{\varepsilon}, \sigma_{0.2}, \sigma_u)$ and $m_{air}\ (T, \dot{\varepsilon}, \sigma_{0.2}, \sigma_u)$.

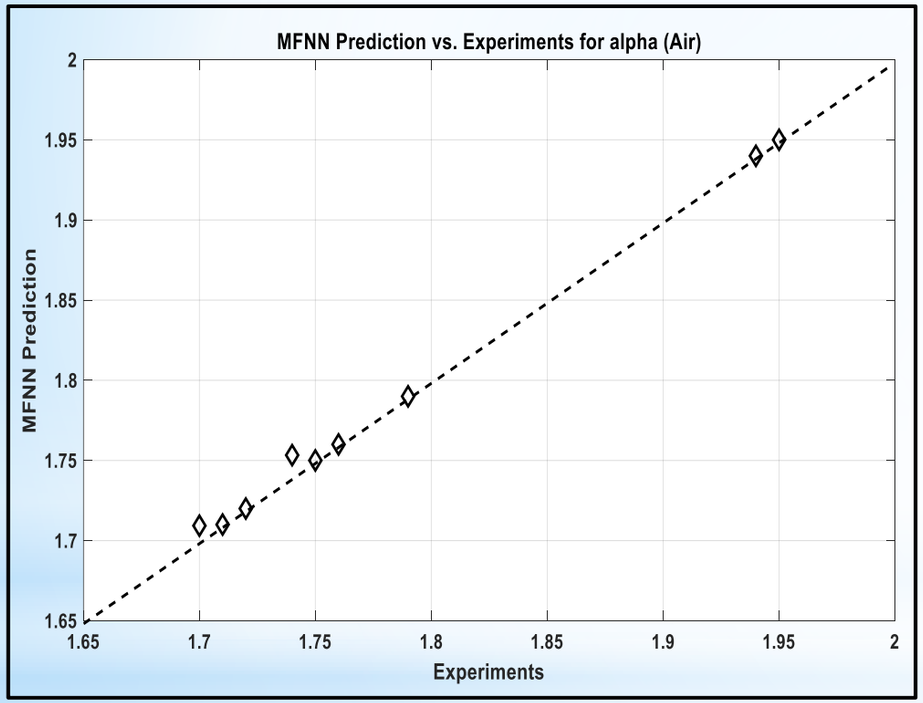

(a)

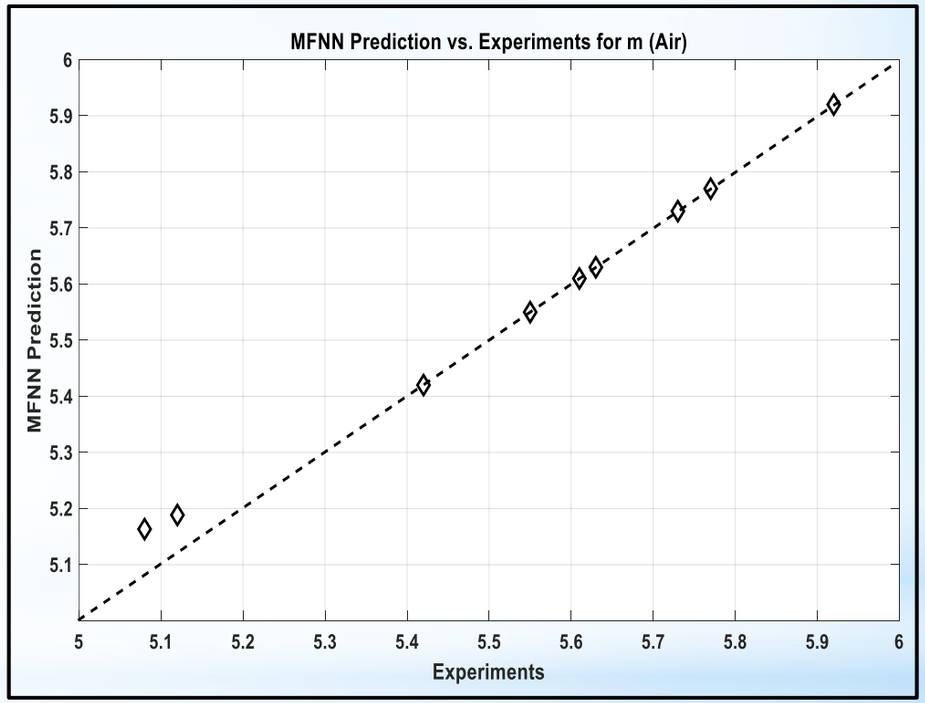

(b)

Predictions of the function $\alpha_{air}\ (T, \dot{\varepsilon}, \sigma_{0.2}, \sigma_u)$ (a) and of the function $m_{air}(T, \dot{\varepsilon}, \sigma_{0.2}, \sigma_u)$ (b) versus experimental values.

II.3 Multilayer feedforward neural network used to model the parameters for ramberg-osgood stress-strain curve equation (4)

- Processing of experimental data obtained for 316L steel **in the liquid lead** environment. After processing the data through the MFNN network methodology, the functions obtained for the R-O coefficients are $\alpha_{lead}\,(T, \dot{\varepsilon}, \sigma_{0.2}, \sigma_u)$ and $m_{lead}\,(T, \dot{\varepsilon}, \sigma_{0.2}, \sigma_u)$.

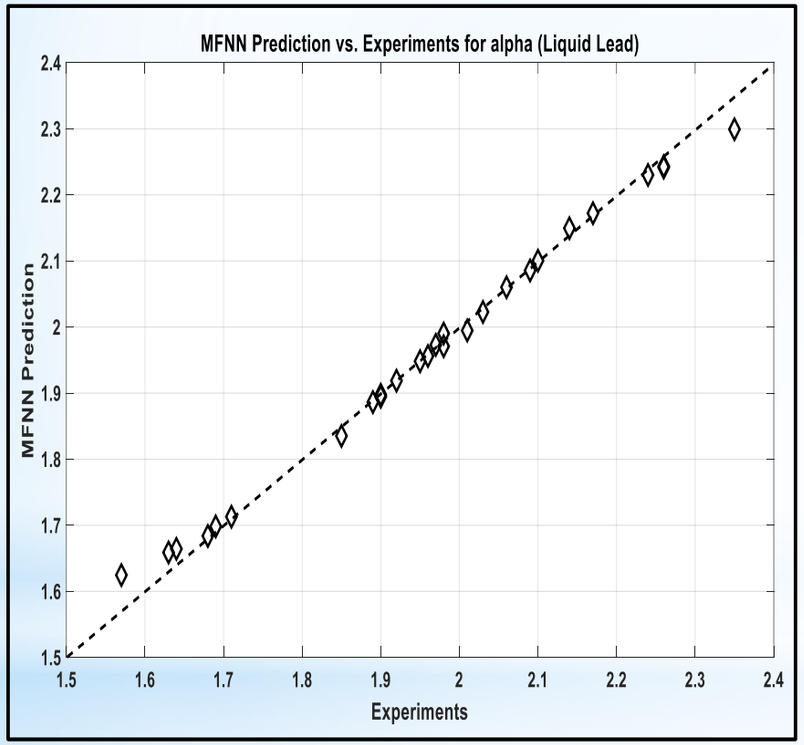

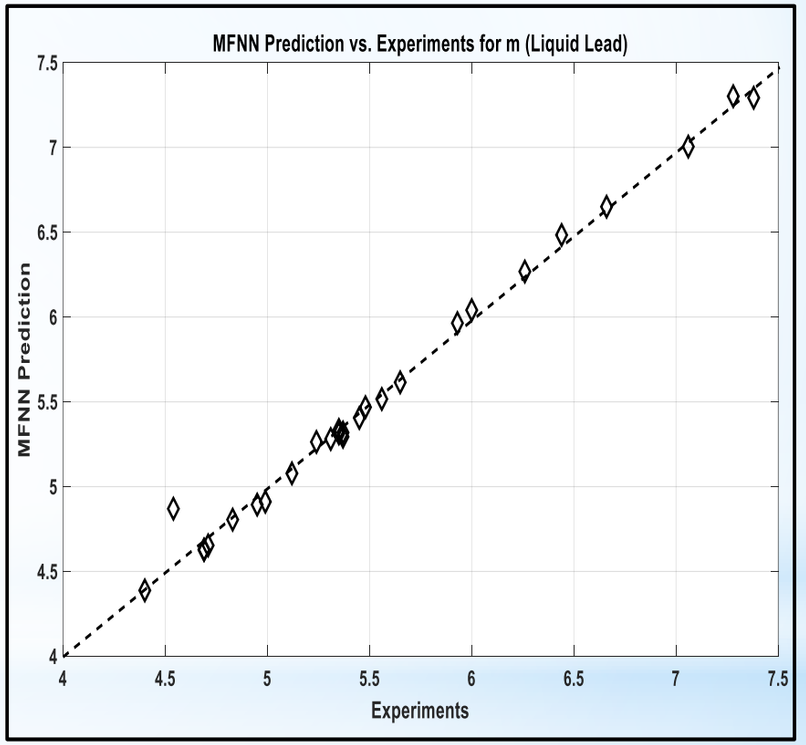

Predictions of the function $\alpha_{lead}\,(T, \dot{\varepsilon}, \sigma_{0.2}, \sigma_u)$ (a) and of the function $m_{lead}\,(T, \dot{\varepsilon}, \sigma_{0.2}, \sigma_u)$(b) versus experimental values.

II.3 Multilayer feedforward neural network used to model the parameters for ramberg-osgood stress-strain curve equation (5)

- Some comments are needed regarding the prediction accuracy of the MFNN model for α and m values compared to the experiments performed in the liquid lead environment.
- It was found from the preliminary analysis a considerable scattering for the values of the parameters α and m, both for the air environment and, especially, for the liquid lead environment.
- However, modelling by the method of artificial neural networks of the MFNN type leads to obtaining fairly accurate prediction functions for α and m, a remarkable fact all the more since they are based on four modelling parameters: temperature, deformation rate, yield stress, the maximum load corresponding to the localized deformation.
- Such modelling, in which several input parameters enter, is very difficult to achieve with the usual fitting methods that are provided in the statistical packages of various programs.

II.4 Application of Ramberg - Osgood MFNN model to assess the stress-strain behaviour of 316l in the air and in the liquid lead environments at the temperature of 375 ºC (1)

For the prediction of the tests carried out in the air environment, we apply the following conditions to obtain the numerical values of the parameters of the Ramberg-Osgood relationship in the analyzed case study: Temperature 375 (*units* ºC); Strain rate $\dot{\varepsilon} = 5\ (units\ 10^{-5}\ s^{-1})$; Yield stress $\sigma_{0.2} = 221\ (units\ MPa)$; Maximum stress at necking $\sigma_u = 497\ (units\ MPa)$.

$$\alpha_{aer}\ (T, \dot{\varepsilon}, \sigma_{0.2}, \sigma_u) = \alpha_{aer}\ (375, 5, 221, 497) = 1.75$$

$$m_{aer}\ (T, \dot{\varepsilon}, \sigma_{0.2}, \sigma_u) = m_{aer}\ (375, 5, 221, 497) = 5.55$$

$$\frac{\varepsilon}{\varepsilon_0} = \frac{\sigma}{\sigma_0} + 1.75 \cdot \left(\frac{\sigma}{\sigma_0}\right)^{5.55}$$

II.4 Application of Ramberg - Osgood mfnn model to assess the stress-strain behaviour of 316l in the air and in the liquid lead environments at the temperature of 375 ºC (2)

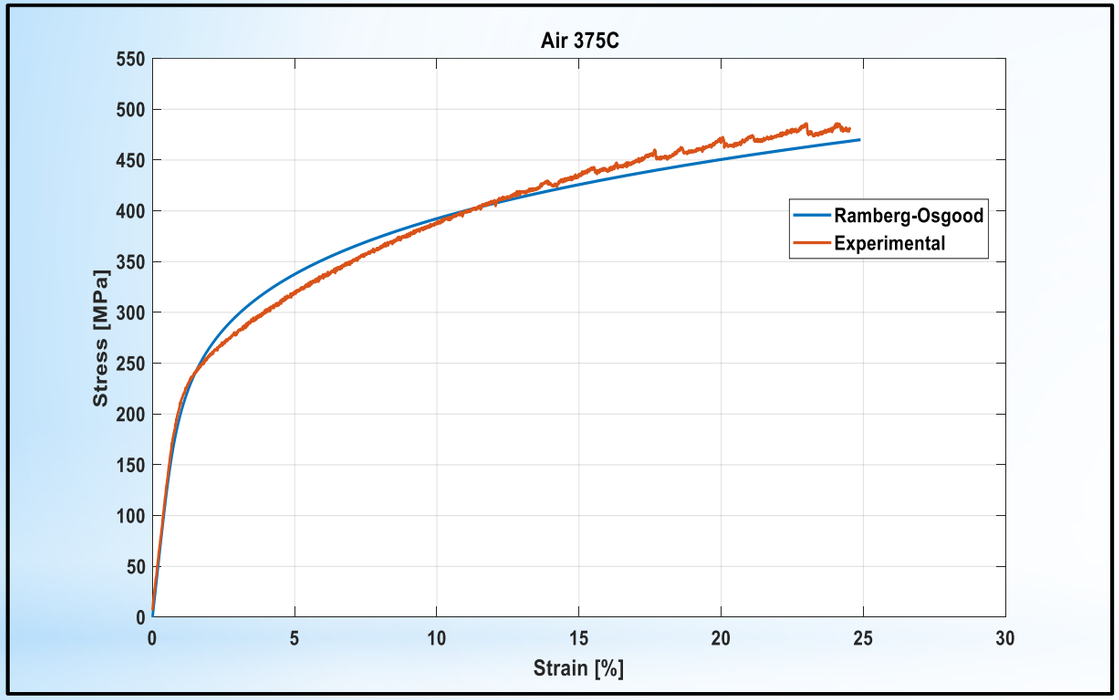

(a)

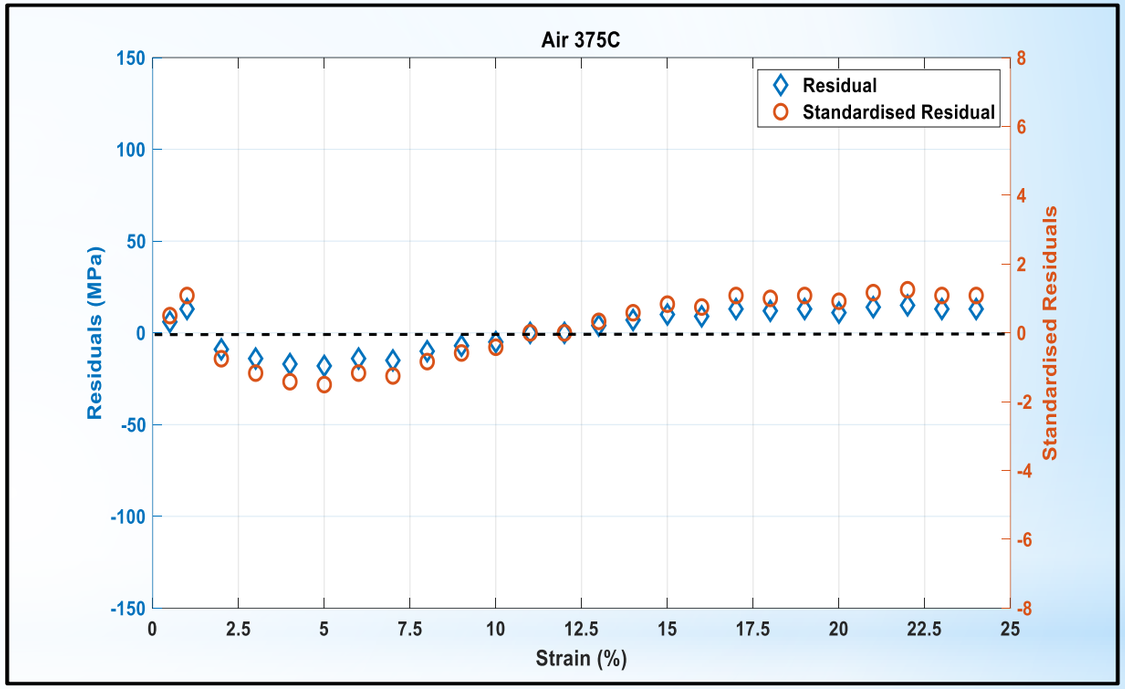

(b)

Comparison between the experimental mechanical stress-strain curve and the Ramberg-Osgood relationship for SSRT tests in the air at 375°C (a) and the residual and standardized residual parameters (b) (S_res<3).

II.4 Application of Ramberg - Osgood mfnn model to assess the stress-strain behaviour of 316l in the air and in the liquid lead environments at the temperature of 375 ºC (3)

For the prediction of the tests carried out in the air environment, we apply the following conditions to obtain the numerical values of the parameters of the Ramberg-Osgood relationship in the analyzed case study: Temperature 375 ($units$ ºC); Strain rate $\dot{\varepsilon} = 5\ (units\ 10^{-5}\ s^{-1})$; Yield stress $\sigma_{0.2} = 209\ (units\ MPa)$; Maximum stress at necking $\sigma_u = 462\ (units\ MPa)$.

$$\alpha_{aer}\ (T, \dot{\varepsilon}, \sigma_{0.2}, \sigma_u) = \alpha_{aer}\ (375, 5, 209, 462) = 1.83$$

$$m_{aer}\ (T, \dot{\varepsilon}, \sigma_{0.2}, \sigma_u) = m_{aer}\ (375, 5, 209, 462) = 5.61$$

$$\frac{\varepsilon}{\varepsilon_0} = \frac{\sigma}{\sigma_0} + 1.83 \cdot \left(\frac{\sigma}{\sigma_0}\right)^{5.61}$$

II.4 Application of Ramberg - Osgood mfnn model to assess the stress-strain behaviour of 316l in the air and in the liquid lead environments at the temperature of 375 ºC (4)

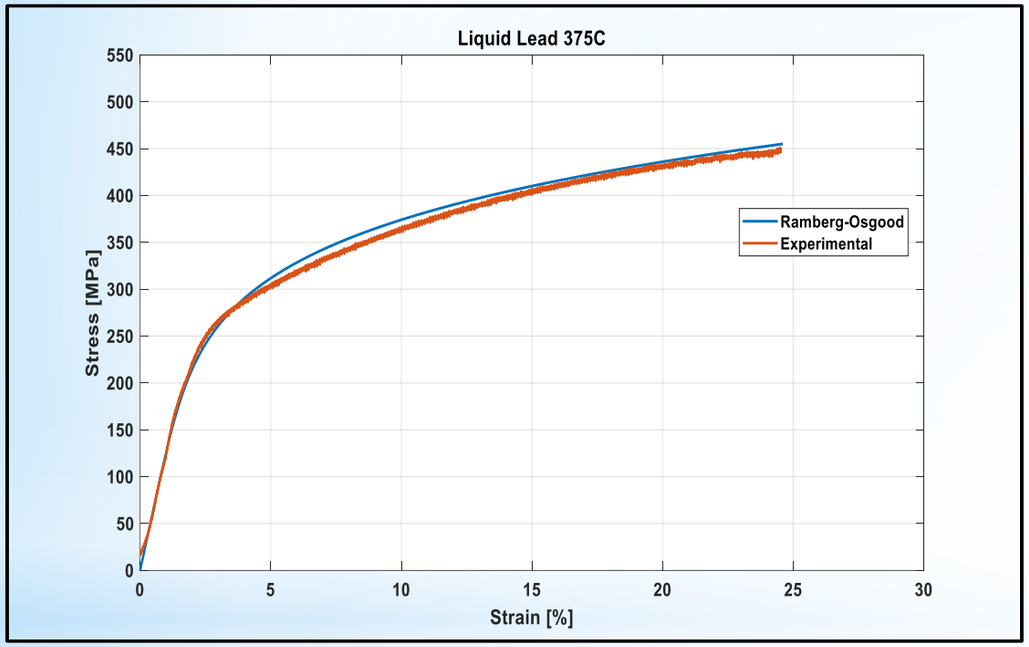

(a)

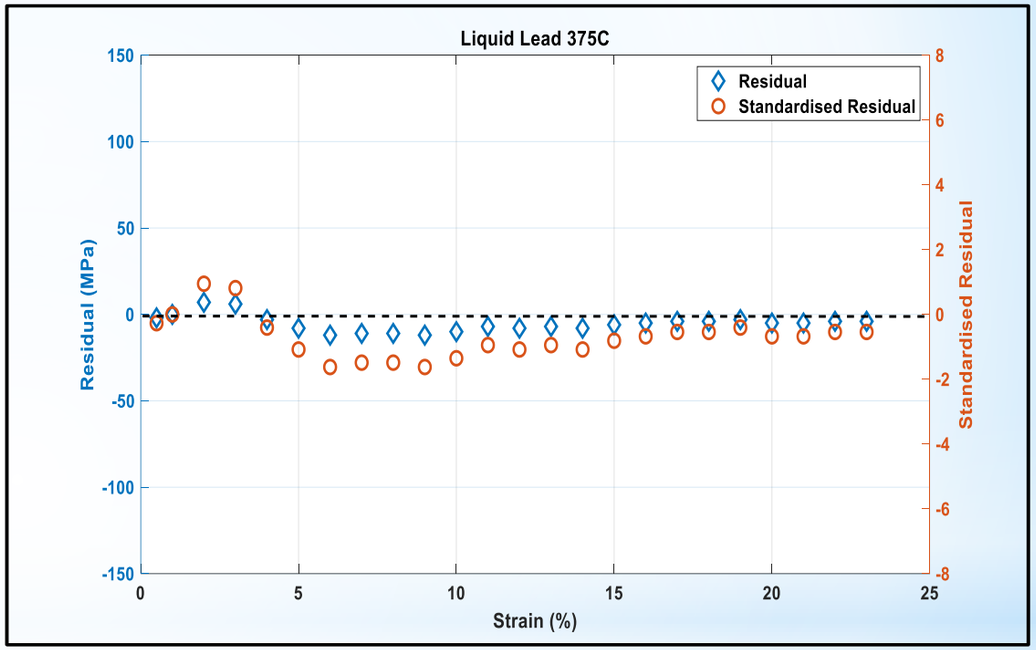

(b)

Comparison between the experimental mechanical stress-strain curve and the Ramberg-Osgood relationship for SSRT tests in the liquid lead at 375°C (a) and the residual and standardized residual parameters (b) ($S_{res} < 3$).

II.4 Application of Ramberg - Osgood mfnn model to assess the stress-strain behaviour of 316l in the air and in the liquid lead environments at the temperature of 375 ºC (4)

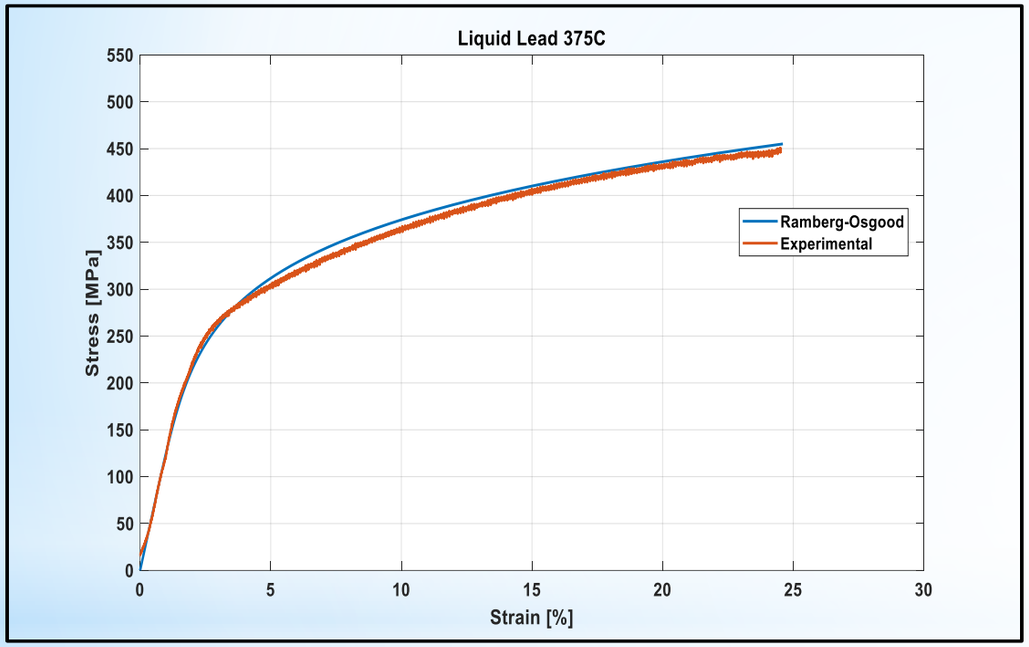

(a)

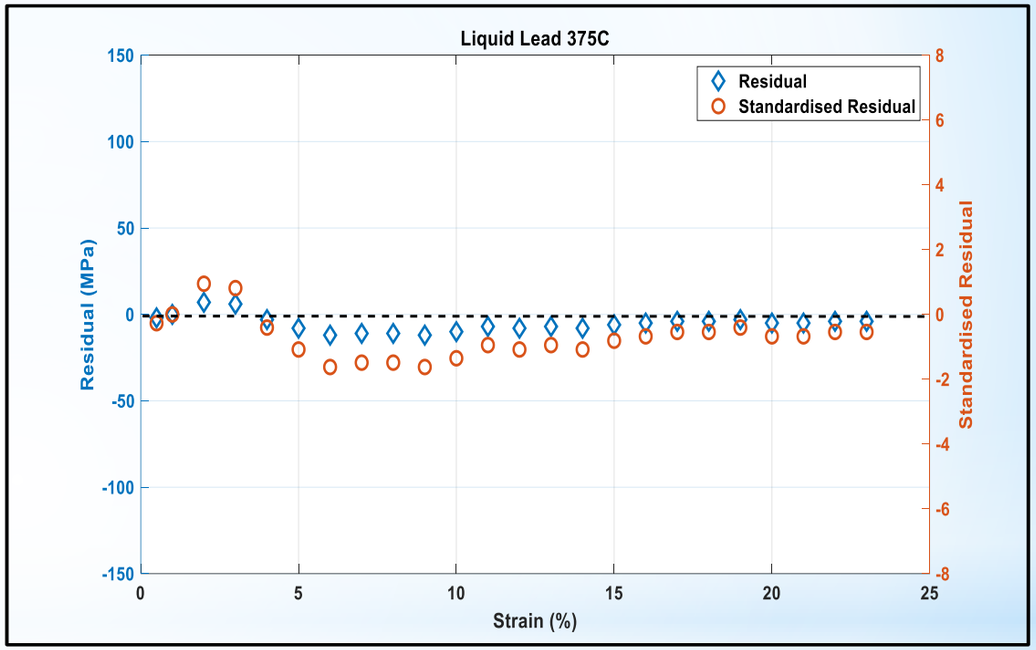

(b)

Comparison between the experimental mechanical stress-strain curve and the Ramberg-Osgood relationship for SSRT tests in the liquid lead at 375°C (a) and the residual and standardized residual parameters (b) ($S_{res} < 3$).

II.4 Application of Ramberg - Osgood mfnn model to assess the stress-strain behaviour of 316l in the air and in the liquid lead environments at the temperature of 375 ºC (5)

2020-11-11 10-21-21.mkv

2020-11-11 08-53-36.mkv

II.5 Normalization data reduction to assess the fracture mechanics behaviour of 316L in the air and in the liquid lead environment (1)

- According with ASTM E 1820 the fracture toughness test (FTT) is usually done by unloading compliance (UC) or potential drop (PD) method, or both at the same time. Both methods require the use of a clip gage extensometer.
- Unfortunately, these conventional methods are not always readily available for tests in the liquid lead. Common clip gage extensometers are difficult to be used because the liquid lead is conductive and chemically attacks the clip gage.
- For this reason, UC and PD methods are not easily applied to FTT in the liquid lead . This forced us to use normalization data reduction (NDR) method to analyze the test results obtained by monotonical load.
- Starting from load-load line displacement data and initial and final crack lengths, the crack opening displacement could be calculated and a J-R curve is obtained. Many studies have proven that normalization data reduction (NDR) method produces comparable results with UC method.
- The procedure of fracture toughness tests in the liquid lead environment should be developed to take into account all the technical difficulties and to provide means for investigation of the effect of the liquid lead on fracture properties.

II.5 Normalization data reduction to assess the fracture mechanics behaviour of 316L in the air and in the liquid lead environment (2)

- The method was used for evaluation only by a few specialized laboratories in the past, recently the method was included in the latest version of the ASTM E 1820-01 standard.
- The fracture mechanics tests were carried out some the steps presented in the ASTM E 1820, adapted for CT samples made of 316L steel.
- The experiments carried out on these CT samples at a temperature of 350 °C, in a molten lead environment, using the LILETIN installation, adapted on the Instron tensile machine.

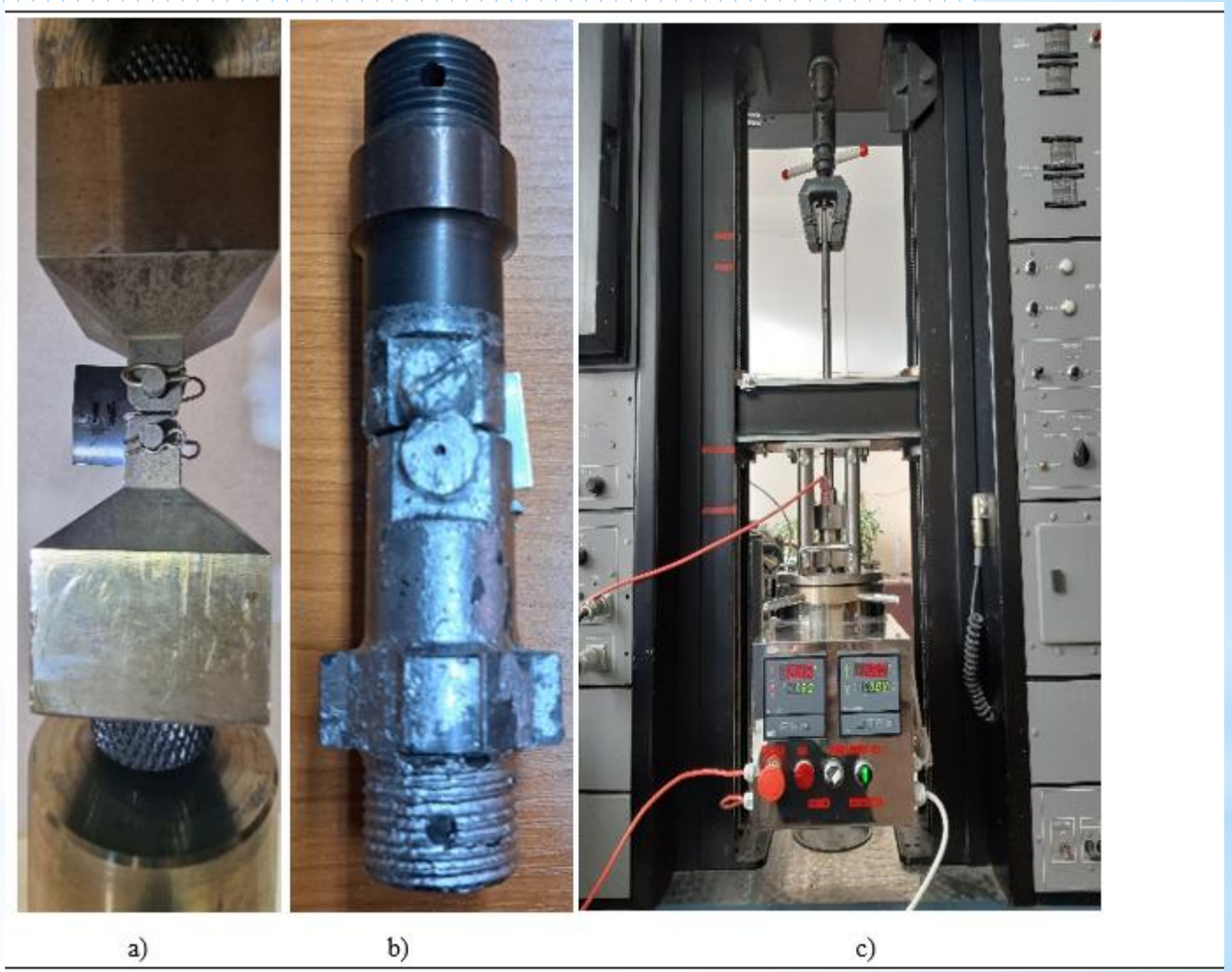

(a) CT specimen assembly for fatigue tests; (b) CT specimen assembly after toughness tests in lead; (c) LILETIN (Instron) installation with liquid lead container for testing

II.5 Normalization data reduction to assess the fracture mechanics behaviour of 316L in the air and in the liquid lead environment (3)

- The experimental data of the type "Force-Displacement on the load line" expressed in kN and mm respectively are saved in files to be used by the normalization program (Normalization_Application) in the MATLAB programming environment.
- They constitute input data and after the program analysis the curves of resistance J-R and the fracture mechanics parameters K_{IC} and J_{IC} are obtained.

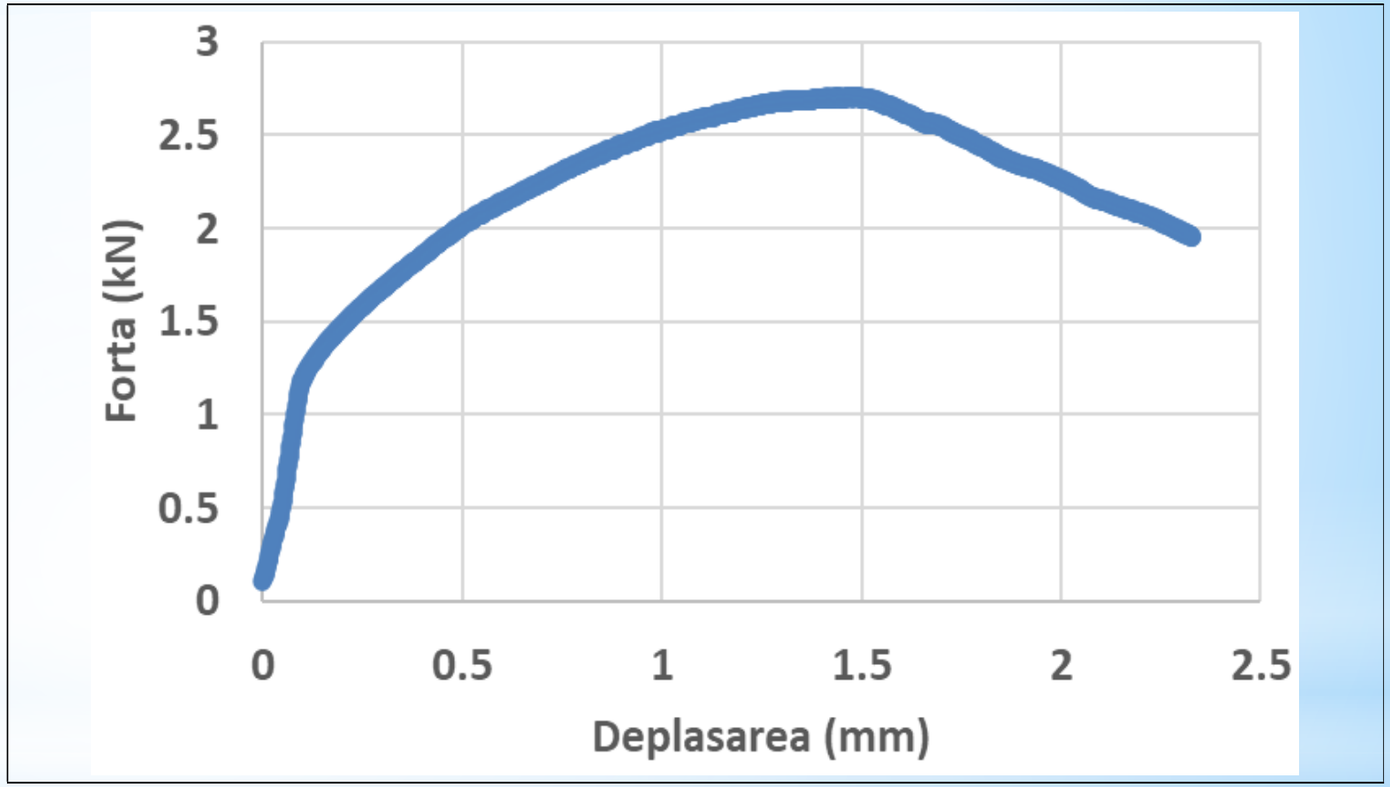

Typical mechanical stress diagram in the fracture mechanics test of a CT sample made of 316L steel

II.5 Normalization data reduction to assess the fracture mechanics behaviour of 316L in the air and in the liquid lead environment (4)

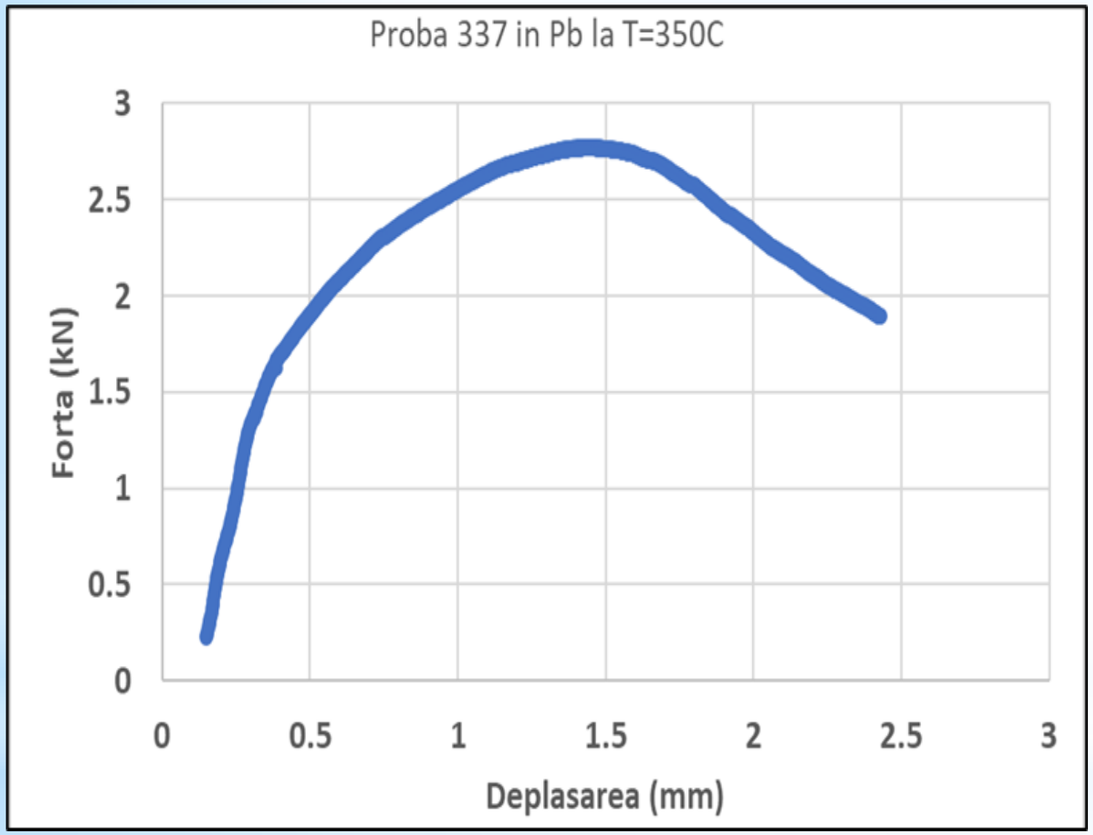

Sample 337: Force-displacement curve on the load line of the CT sample during the fracture mechanics test

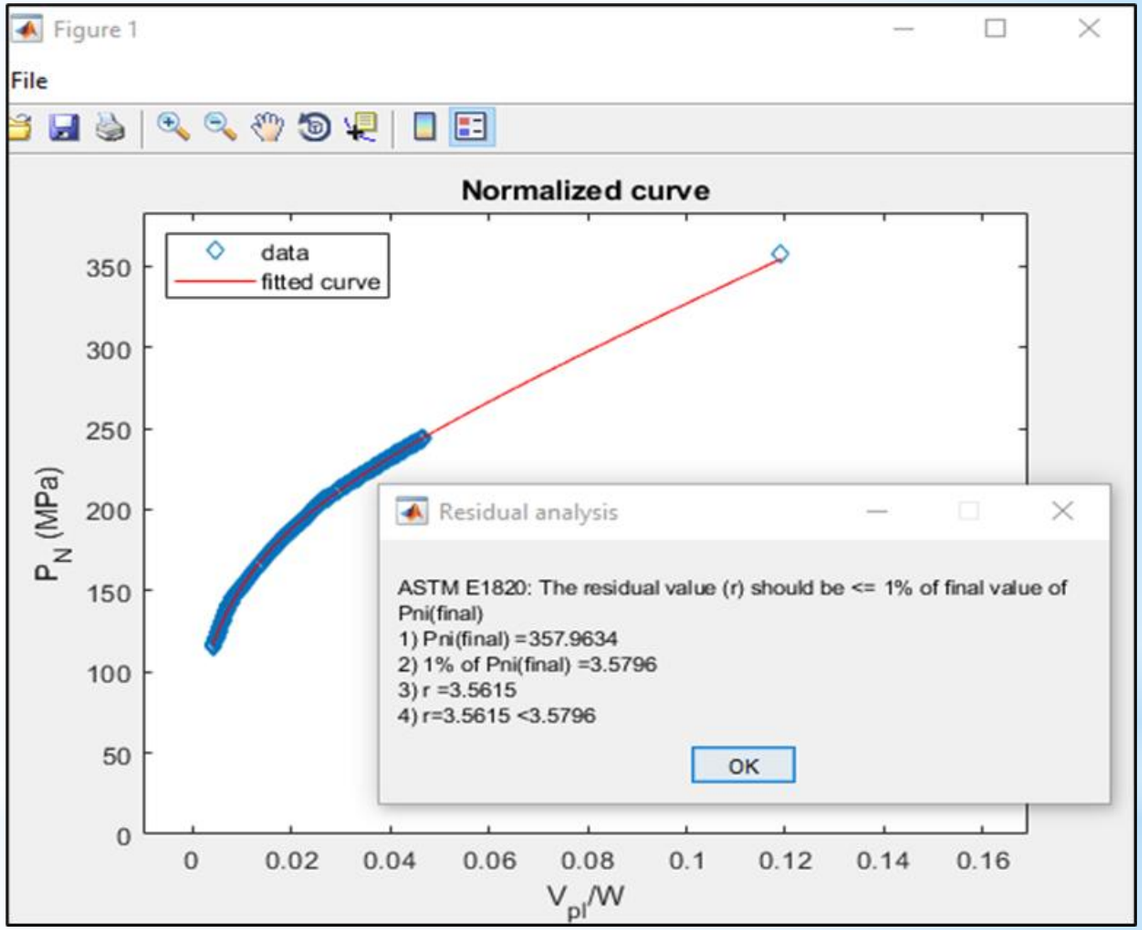

Sample 337: CT sample normalization curve and convergence values according to ASTM E1820

II.5 Normalization data reduction to assess the fracture mechanics behaviour of 316L in the air and in the liquid lead environment (4)

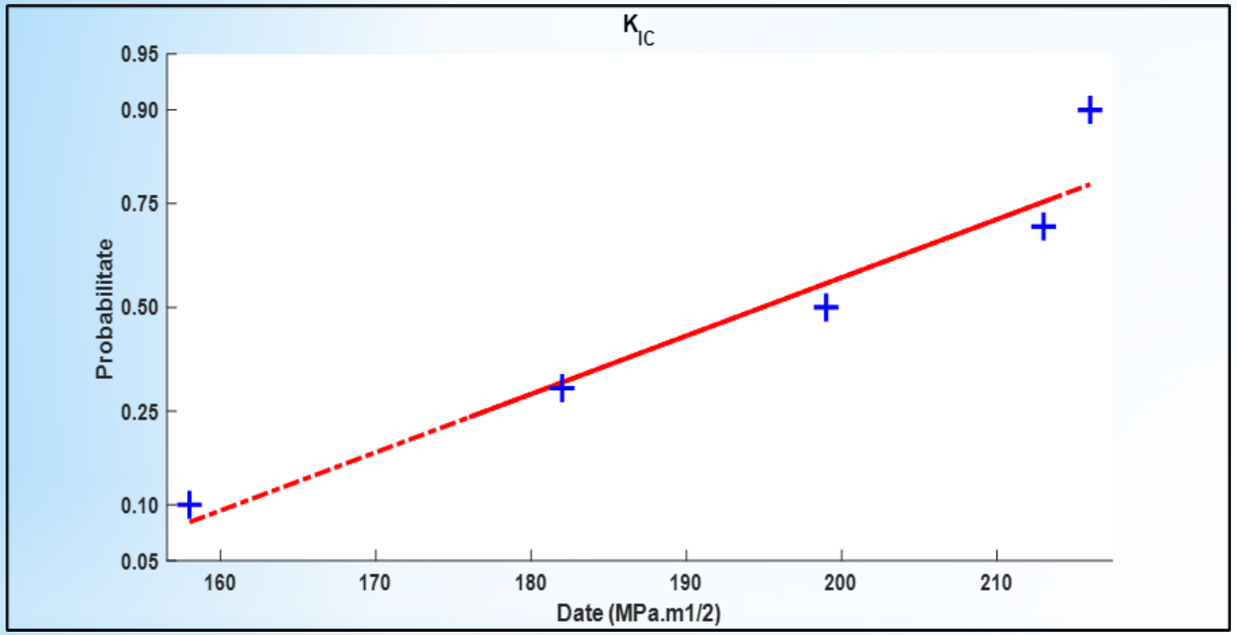

The agreement test regarding the normal distribution of the values obtained for the K_{IC} fracture toughness of 316L steel in molten lead, T=350°C

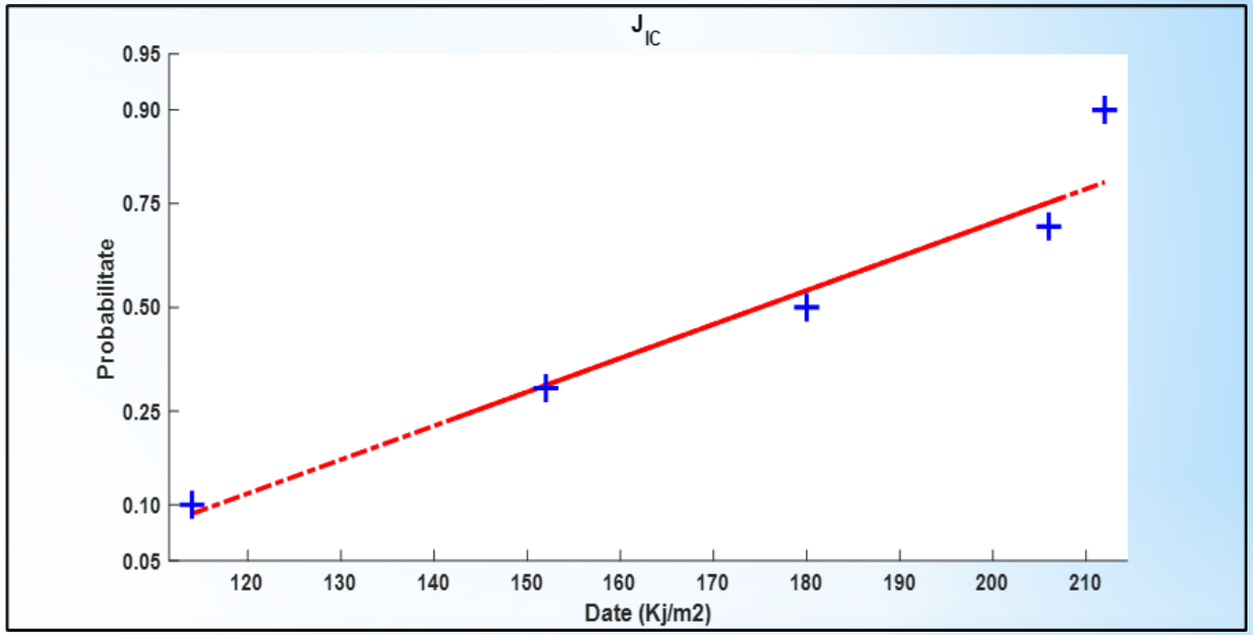

The agreement test regarding the normal distribution of the values obtained for the J_{IC} fracture toughness of 316L steel in molten lead, T=350°C

II.5 Normalization data reduction to assess the fracture mechanics behaviour of 316L in the air and in the liquid lead environment (5)

- In the statistical analysis of the data obtained for the fracture mechanics parameters K_{IC} and J_{IC} , a confidence coefficient α=10% will be used.
- For t-Student distribution, the confidence interval, bilaterally symmetric, containing the real value of the parameter μ, with probability (1-α), is:

$$\left[\bar{x} + t_{\frac{\alpha}{2},n-1} \cdot {}^{s}/_{\sqrt{n}} \leq \mu \leq \bar{x} - t_{\frac{\alpha}{2},n-1} \cdot {}^{s}/_{\sqrt{n}}\right]$$

- For the toughness parameter K_{IC} the following results are obtained:

$$170.74\ MPa\sqrt{m} \leq K_{IC} \leq 216.46\ MPa\sqrt{m}$$

- For the toughness parameter K_{IC} the following results are obtained:

$$134.16\ \frac{kJ}{m^2} \leq J_{IC} \leq 211.44\ \frac{kJ}{m^2}$$

Conclusions

- The use of heavy liquid metals, and especially of lead-cooled or lead-alloy-cooled (primarily LBE) fast reactor (LFR) concepts of Generation IV requires an assessment of their compatibility with structural materials under the fast-neutron spectrum typical of fast reactors.
- Because the 316L austenitic stainless steel has been preselected for the design of future European transmutation facilities (EFIT, XT-ADS) and eventually also for the lead-cooled fast reactor, the effect of LBE or lead on the mechanical behavior of these steels is being extensively investigated in Europe and worldwide, and results are available, but they are not yet exhaustive.
- Today, and in spite of a lack of quantitative results on fatigue and fracture, based on analysis of the data collected on the tensile and fatigue tests, the question of the susceptibility to LME (embrittlement) of structural materials in contact with lead or LBE can be addressed, particularly how to proceed from the metallurgical and chemical points of view to prevent LME.
- Information on fracture mechanics, from fracture toughness to crack growth behavior in contact with LBE, does not exist.
- For these reasons, the presentation showed several aspects of the studies that are underway within RATEN ICN regarding the behavior of structural materials in contact with molten lead.

References

1. Pascal Yvon, Structural Materials for Generation IV Nuclear Reactors, Woodhead Publishing Series in Energy: Number 106, Copyright © 2017 Elsevier Ltd. All rights reserved.
2. K.L. Murty , I. Charit, Structural materials for Gen-IV nuclear reactors: Challenges and opportunities, Journal of Nuclear Materials 383 (2008) 189–195
3. ***, Handbook on Lead-bismuth Eutectic Alloy and Lead Properties, Materials Compatibility, Thermal-hydraulics and Technologies, 2015 Edition, © OECD 2015 NEA. No. 7268
4. Dan Gabriel Cacuci (Ed.), Handbook of Nuclear Engineering, Chapter 23 Lead-Cooled Fast Reactor (LFR)Design: Safety, Neutronics, Thermal Hydraulics, Structural Mechanics, Fuel, Core, and Plant Design © Springer Science+Business Media LLC 2010

I want to thank my colleagues Alexandru NITU and Livia STOICA for helping me with materials from their works to prepare this presentation, as well as my colleagues from the Thermomechanical and Microstructural Properties Team for carrying out the tests in good conditions!

Thank you for your attention!